Mathematical Biosciences and Engineering

https://www.aimspress.com/journal/mbe

MBE, 23(6): 1622–1650.
DOI: 10.3934/mbe.2026059
Received: 07 February 2026
Revised: 17 April 2026
Accepted: 21 April 2026
Published: 30 April 2026

Research article

A nonlinear time-delay modeling case study of Tuberculosis transmission in Algeria: 1990–2024

Nadjla Abidat[1], Akhil Kumar Srivastav[2,*], Nico Stollenwerk[2], Abderrazak NABTi[1] and Maíra Aguiar[2,3,*]

[1] Laboratory of mathematics, informatics and systems (LAMIS), Echahid Cheikh Larbi Tebessi University, Tebessa, 12002, Algeria

[2] Basque Center for Applied Mathematics, Alameda de Mazarredo, Bilbao, 48009, Bizkaia, Spain

[3] Ikerbasque, Basque Foundation for Science, Bizkaia, Spain

* **Correspondence:** Email: asrivastav@bcamath.org, maguiar@bcamath.org.

Abstract: This study develops a nonlinear time-delay mathematical model to investigate the transmission dynamics of tuberculosis in Algeria over the period 1990–2024. The model explicitly incorporates a delay representing the incubation period between infection and the onset of infectiousness, which significantly affects system behavior by potentially inducing instability and oscillatory dynamics. In particular, increasing the delay can destabilize the endemic equilibrium and lead to periodic outbreaks through Hopf bifurcation. The basic reproduction number $\mathcal{R}_0$ is derived, and rigorous analysis establishes the local and global stability conditions for both disease-free and endemic equilibria. Sensitivity analysis identifies key epidemiological parameters influencing $\mathcal{R}_0$, providing insight into effective intervention strategies. From a public health perspective, the results highlight that reducing diagnostic delays and improving timely treatment can stabilize disease dynamics and prevent recurrent outbreaks. Numerical simulations, calibrated with Algerian tuberculosis data from 1990 to 2024, support the theoretical findings and demonstrate the critical role of delay effects in shaping tuberculosis transmission and control.

Keywords: Tuberculosis; time-delay; reproduction number; stability analysis; sensitivity analysis; data analysis

1. Introduction

Tuberculosis (TB) is defined as a chronic infectious disease caused by *Mycobacterium tuberculosis*, and it is primarily transmitted through airborne droplets released by individuals with active pulmonary infection. TB is one of the oldest and most complex infectious diseases worldwide, and it continues

to pose a major public health challenge despite significant advances in diagnostic tools, treatment strategies, and epidemiological surveillance programs. According to the latest reports from the World Health Organization, TB is ranked among the leading causes of death from infectious diseases, with millions of cases reported annually particularly in low- and middle-income countries where social, economic, and health conditions facilitate its spread [1]. TB transmission is characterized by complex epidemiological features, most notably latent infection, the long interval between exposure and the onset of symptoms, difficulties in early detection, and the possible emergence of drug-resistant strains, all of which make eliminating the disease a long-term goal [2].

Given the great complexity of TB transmission, mathematical modeling has emerged as a crucial tool for understanding disease dynamics, analyzing transmission mechanisms, and assessing the impact of health interventions [3,4]. Over the past decade, significant progress has been made beyond the classical deterministic susceptible, infectious, and removed (SIR) and susceptible, exposed, infectious, and removed (SEIR) models, with the development of age-structured models, reinfection models, multi stage infection models, and agent-based frameworks that capture heterogeneity in contact patterns and disease progression [5, 6]. Recent studies have also introduced fractional-order and delay differential equation (DDE) models to represent more realistic biological processes, especially latency, long progression times, and memory effects in transmission dynamics [7–9]. Traditional TB models often assume instantaneous transitions between compartments, overlooking natural biological delays such as incubation time, delayed onset of symptoms, and delays in diagnosis and treatment. These delays are fundamental components capable of altering system stability and generating oscillatory behavior when critical thresholds are crossed [10, 11]. Modern DDE-based TB models address these limitations by explicitly incorporating such delays, offering better agreement with epidemiological data and more accurate predictions [12, 13]. Moreover, nonlinear incidence functions including saturated or behavioral-based incidence have gained increasing attention due to their ability to reflect reductions in transmission resulting from healthcare constraints or behavioral changes during outbreaks [14, 15]. Recent analyses show that these nonlinearities can generate rich dynamical behavior, modify the basic reproduction number $\mathcal{R}_0$, and play a key role in the emergence of Hopf bifurcations [16].

Despite previous scientific efforts, clear research gaps still remain. To date, there are no mathematical models that incorporate both nonlinear incidence functions and time delays while simultaneously being calibrated to real epidemiological data from Algeria. This absence limits the understanding of how delay effects influence system stability and the emergence of oscillations through Hopf bifurcation. Furthermore, there is a noticeable lack of studies that connect advanced theoretical models with field data from affected countries, including Algeria, highlighting the need for more accurate and realistic modeling approaches.

TB holds particular importance in Algeria, where it remains a disease requiring continuous monitoring and reinforcement of public health programs. According to official reports from the Algerian Ministry of Health and the World Health Organization, the country has recorded fluctuating incidence rates over the past two decades, with case numbers rising and falling in response to social, health, and economic factors [17–19]. Algeria has implemented several TB control programs, including the expansion of early detection systems, the adoption of the directly observed therapy, short-course (DOTS) strategy [20], improvements in drug supply chains, and the strengthening of diagnostic centers. Nevertheless, several challenges persist, such as delayed diagnosis, disparities in healthcare quality across regions, and the emergence of some drug-resistant TB cases [19]. Studying the basic reproduction

number $\mathcal{R}_0$ of TB in Algeria is essential for evaluating the infection's transmissibility and determining the effectiveness of control programs. Integrating mathematical models calibrated with Algerian data provides deeper insight into disease trends and possible future scenarios, especially considering the time delays associated with transmission, diagnosis, and treatment delays that directly influence disease dynamics in the Algerian population.

These studies [21–23] explore advanced epidemic models incorporating factors such as government intervention, vaccination, and healthcare limitations. They demonstrate how real-world complexities can lead to rich dynamics, including oscillations, bifurcations, and chaos, highlighting the importance of realistic modeling for understanding and controlling disease spread.

In this work, we develop a nonlinear mathematical model for tuberculosis transmission that incorporates a time delay representing the natural progression from initial infection to the onset of infectiousness. The model is based on a standard incidence formulation, where the transmission process is determined by the effective contact between susceptible and infectious individuals relative to the total population size. We derive both the disease-free and endemic equilibrium points and compute the basic reproduction number $\mathcal{R}_0$. We also perform a detailed local stability analysis. In addition, we identify the conditions under which oscillatory behavior arises through a Hopf bifurcation. Numerical simulations, calibrated using real epidemiological data from Algeria, are presented to support the analytical results and to illustrate the effect of standard incidence and the time delay between infection and the onset of infectiousness on the dynamics of disease spread. Overall, this work provides a comprehensive mathematical framework for understanding tuberculosis transmission in Algeria and for evaluating the impact of progression delays on control strategies.

2. Formulation of the model

To describe the transmission dynamics of tuberculosis, we develop a delayed epidemic model that divides the population into five epidemiological compartments, as illustrated in Figure 1. These compartments are: the susceptible class $S_1(t)$; the newly infected individuals with primary infection $I_1(t)$; the treated individuals under therapy $R(t)$; the secondary susceptible class $S_2(t)$, which consists of individuals who have lost their post-treatment immunity; and the reinfected (secondary infection) class $I_2(t)$. The total population at time t is denoted by N, and its evolution is determined by natural birth and death processes.

- New individuals enter the population through natural recruitment at rate μN, and all compartments are subject to natural mortality at rate μ.
- Infection occurs through effective contact between susceptible individuals and the two infectious classes, I_1 and I_2, at transmission rate β.
- A time delay τ is incorporated in the primary infection pathway to capture the latent (incubation) period of tuberculosis, during which individuals are infected with *Mycobacterium tuberculosis* but are not yet infectious. This delay reflects the well-established biological feature that TB has a prolonged and variable latency phase, which can range from weeks to years before progression to active, transmissible disease. Including τ therefore improves model realism by accounting for the slow progression from infection to active TB, a key characteristic distinguishing TB from acute infections. This approach is widely supported in the literature [24–26], where delay terms are used to represent latency and its impact on transmission dynamics.

- The parameter ϕ represents the relative infectiousness of individuals in the reinfected class I_2 compared with those in the primary infection class I_1, thereby capturing possible differences in transmission potential.
- In tuberculosis (TB) modeling, individuals in the primary infection class $I_1(t)$ who recover and enter the treatment class R(t) at rate γ are typically assumed to have temporary partial immunity, not lifelong protection. The transition from $R(t)$ to the secondary susceptible class $S_2(t)$ is therefore defined by a temporary cross immunity rate α. They may also experience reactivation or incomplete recovery, returning to the primary infection class $I_1(t)$ at rate ν. Individuals in the secondary susceptible class $S_2(t)$ are vulnerable to immediate reinfection, without delay, since no latent period is assumed following immunity loss.

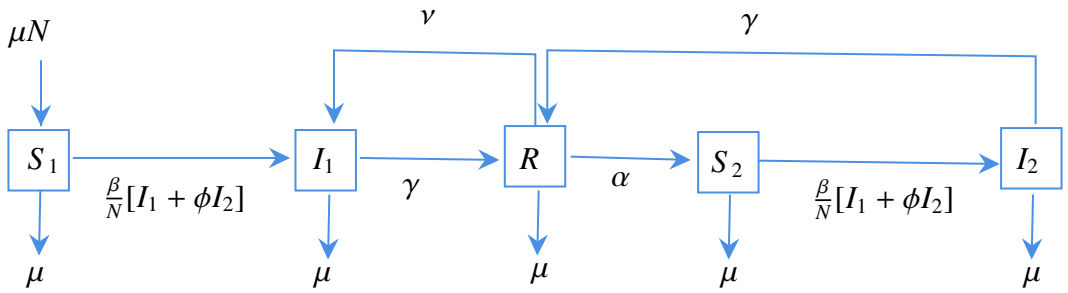

Figure 1. Diagram of TB transmission dynamics.

Based on these assumptions, the dynamics of the system are described by the following set of delay differential equations

$$\begin{cases} \dfrac{dS_1(t)}{dt} = \mu(N - S_1(t)) - \beta\dfrac{S_1(t-\tau)}{N}\left[I_1(t-\tau) + \phi I_2(t-\tau)\right], \\ \dfrac{dI_1(t)}{dt} = \beta\dfrac{S_1(t-\tau)}{N}\left[I_1(t-\tau) + \phi I_2(t-\tau)\right] - (\gamma+\mu)I_1(t) + \nu R(t), \\ \dfrac{dR(t)}{dt} = \gamma I_1(t) + \gamma I_2(t) - (\nu+\alpha+\mu)R(t), \\ \dfrac{dS_2(t)}{dt} = \alpha R(t) - \mu S_2(t) - \beta\dfrac{S_2(t)}{N}\left[I_1(t) + \phi I_2(t)\right], \\ \dfrac{dI_2(t)}{dt} = \beta\dfrac{S_2(t)}{N}\left[I_1(t) + \phi I_2(t)\right] - (\mu+\gamma)I_2(t). \end{cases} \tag{2.1}$$

The initial conditions for system (2.1) take the form

$$S_1(\varphi) = \psi_1(\varphi) > 0,\ I_1(\varphi) = \psi_2(\varphi) > 0,\ R(\varphi) = \psi_3(\varphi) > 0,\ S_2(\varphi) = \psi_4(\varphi) > 0,\ I_2(\varphi) = \psi_5(\varphi) > 0. \tag{2.2}$$

On $\varphi \in [-\tau, 0]$, and $(\psi_1, \psi_2, \psi_3, \psi_4, \psi_5)^T \in C\left(\max[-\tau, 0], \mathbb{R}^5\right)$ as a Banach space of continuous function from $[-\tau, 0]$ into $\mathbb{R}^5$.

3. Mathematical analysis

This section focuses on examining the fundamental qualitative properties of the system, specifically the positivity and boundedness of its solutions. We begin by establishing that the five state variables

remain non-negative for all future time, ensuring that the model is consistent with biological reality. We then identify the feasible region of the system

$$\Omega = \left\{(S_1, I_1, R, S_2, I_2) \in \mathbb{R}^5_+ : 0 \leq S_1, I_1, R, S_2, I_2 \leq C\right\}, \tag{3.1}$$

and prove that this region is closed and positively invariant under the system dynamics, so that all trajectories remain confined within it. These results form an essential foundation for the subsequent stability and dynamical analysis of the model.

Theorem 1. *The feasible region defined by* (3.1) *is positively invariant for the proposed model. In particular, every solution that begins in this region remains inside it for all $t \geq 0$, for any non-negative delay parameters appearing in the system.*

Proof. To establish the validity of Theorem 1, we begin by demonstrating the positivity of the solutions. By applying the variation of constants formula together with a step-by-step integration approach, and integrating the first equation of the model system (2.1)–(2.2) over the interval from 0 to t for $0 < t \leq \tau$, we obtain the following result

$$S_1(t) > S_1(0)e^{-\mu t} \times e^{\int_0^t S_1(\varepsilon-\tau)H(I_1(\varepsilon-\tau),I_2(\varepsilon-\tau),S_1(\varepsilon))d\varepsilon},$$

with

$$H\big(I_1(\varepsilon-\tau),\, I_2(\varepsilon-\tau),\, S_1(\varepsilon)\big) = \beta\frac{\big[I_1(\varepsilon-\tau) + \phi I_2(\varepsilon-\tau)\big]}{NS_1(\varepsilon)}.$$

It is immediate from the initial conditions that $S_1(t) > 0$ for every $t \in [0,\, \tau]$. To extend this property beyond the initial interval, we integrate the first equation of the system from $\varepsilon = \tau$ to $\varepsilon = t$, for $\tau < t \leq 2\tau$. This yields

$$S_1(t) > S_1(0)\, e^{-\mu t}\, \exp\left(\int_\tau^t S_1(\varepsilon-\tau)H\big(I_1(\varepsilon-\tau),\, I_2(\varepsilon-\tau),\, S_1(\varepsilon)\big)\, d\varepsilon\right).$$

Since the exponential term is strictly positive, it follows that $S_1(t) > 0$ for all $t \in [\tau,\, 2\tau]$. Repeating the same argument over successive intervals of length τ establishes, by induction, that the positivity of $S_1(t)$ holds for every $t > 0$. Consequently, the susceptible population never reaches zero or becomes negative throughout the evolution of the system.

By applying the same reasoning to the remaining equations of the model, one can systematically verify that all state variables remain positive for every $t > 0$, provided that the initial conditions are positive. As a result, the system's trajectories stay within a biologically meaningful and bounded region. Hence, the model preserves positivity and admits unique solutions that remain well defined and biologically relevant for all future times.

In order to verify the boundedness of the system, consider the total population $N(t)$. From the model, we observe that

$$\frac{dN(t)}{dt} = \frac{dS_1(t)}{dt} + \frac{dI_1(t)}{dt} + \frac{dR(t)}{dt} + \frac{dS_2(t)}{dt} + \frac{dI_2(t)}{dt} = 0,$$

which implies that $N(t)$ remains constant for all $t \geq 0$. Hence,

$$N(t) = C,$$

where C is a positive constant determined by the initial population size. Since

$$N(t) = S_1(t) + I_1(t) + R(t) + S_2(t) + I_2(t),$$

it follows directly that each individual compartment satisfies

$$0 \leq S_1(t),\ I_1(t),\ R(t),\ S_2(t),\ I_2(t) \leq C \quad \text{for all } t \geq 0.$$

Thus, all state variables are uniformly bounded by the constant C, completing the proof of the theorem. □

3.1. Analysis of the model equilibria

In this section, we present the equilibrium points of system (2.1)-(2.2) and explain how they are obtained, since studying these equilibrium points is essential for understanding the long-term behavior of the model and determining whether the infection will disappear or persist within the population.

For the system (2.1)-(2.2), its disease-free equilibrium is given by

$$E^0 = (N, 0, 0, 0, 0),$$

where the number of susceptible individuals remains constant, while all other compartments are at their trivial state.

The endemic equilibrium E^*, on the other hand, corresponds to a situation in which the infection persists at steady levels. Obtaining this equilibrium requires first introducing the basic reproduction number $\mathcal{R}_0$, which helps simplify the algebraic relations used to determine the equilibrium values.

3.2. Basic reproduction number

The basic reproduction number, denoted by $\mathcal{R}_0$, represents the average number of secondary infections generated by a single infectious individual introduced into a fully susceptible population. It serves as a key indicator of the epidemic potential of the disease and plays a central role in the qualitative analysis of infectious disease models, as it helps determine whether the infection will die out or persist in the community. Having established the disease free equilibrium (DFE,) we now compute the basic reproduction number $\mathcal{R}_0$ using the next-generation approach [27].

To apply this method, we extract from system (2.1)-(2.2) ($\tau = 0$) the equations corresponding to the state variables involved in the transmission dynamics. Let $\mathbf{x}(t)$ denote the vector gathering these variables. The corresponding subsystem can be written in vector form as

$$\dot{\mathbf{x}}(t) = \mathcal{F}(\mathbf{x}(t)) - \mathcal{V}(\mathbf{x}(t)),$$

where

$$\mathcal{F}(\mathbf{x}(t)) = \begin{pmatrix} \frac{\beta S_1(t)}{N}[I_1(t) + \phi I_2(t)] \\ 0 \\ \frac{\beta S_2(t)}{N}[I_1(t) + \phi I_2(t)] \end{pmatrix}, \qquad \mathcal{V}(\mathbf{x}(t)) = \begin{pmatrix} (\gamma + \mu)I_1(t) - \nu R(t) \\ -\gamma I_1(t) - \gamma I_2(t) + (\nu + \alpha + \mu)R(t) \\ (\mu + \gamma)I_2(t) \end{pmatrix}, \quad (3.2)$$

then

$$F = \begin{pmatrix} \beta & 0 & \phi\beta \\ 0 & 0 & 0 \\ 0 & 0 & 0 \end{pmatrix}, \qquad V = \begin{pmatrix} (\gamma+\mu) & -\nu & 0 \\ -\gamma & (\nu+\alpha+\mu) & -\gamma \\ 0 & 0 & (\mu+\gamma) \end{pmatrix}, \tag{3.3}$$

Therefore, the expression of the basic reproduction number $\mathcal{R}_0$ of system (2.1)–(2.2) is given by.

$$\mathcal{R}_0 = \rho(FV^{-1}) = \frac{\beta(\nu+\alpha+\mu)}{\gamma(\alpha+\mu)+\mu(\nu+\alpha+\mu)}. \tag{3.4}$$

The basic reproduction number $\mathcal{R}_0$ represents the average number of secondary infections generated by a single infectious individual in a fully susceptible population. It is derived using the next-generation matrix approach, where $\rho(FV^{-1})$ denotes the spectral radius. In the expression

$$\mathcal{R}_0 = \frac{\beta(\nu+\alpha+\mu)}{\gamma(\alpha+\mu)+\mu(\nu+\alpha+\mu)},$$

the numerator $\beta(\nu+\alpha+\mu)$ captures the effective transmission potential, combining the infection rate β with transitions related to progression (ν), loss of immunity (α), and natural death (μ). The denominator $\gamma(\alpha+\mu)+\mu(\nu+\alpha+\mu)$ represents the overall removal processes from the infectious pathway, including recovery (γ) and natural mortality. Thus, $\mathcal{R}_0$ reflects the balance between infection generation and removal mechanisms and serves as a threshold parameter: If $\mathcal{R}_0 < 1$, the disease dies out, whereas if $\mathcal{R}_0 > 1$, the infection persists and may lead to an endemic state.

3.3. Forward sensitivity analysis

Sensitivity analysis enables the researcher to ascertain the impact of parameters inside the model.

This approach assesses the variation in outcomes resulting from changes in input factors. In this work, we examine the impact of variation on the fundamental reproduction number. Parameters in the formulation of the fundamental reproduction number represent key biological and epidemiological processes governing disease transmission, progression, and recovery. The sensitivity may be quantified by the partial derivative about the parameters of $\mathcal{R}_0$, denoted by the notation, $\Gamma_p^{\mathcal{R}_0} = \frac{\partial \mathcal{R}_0}{\partial p}\frac{p}{\mathcal{R}_0}$, where p represents any parameter in the expression of $\mathcal{R}_0$ [28].

The parameters included in the formulation of the fundamental reproduction number are $\beta, \gamma, \mu, \alpha, \mu$. Starting with β

$$\Gamma_\beta^{\mathcal{R}_0} = \frac{\partial \mathcal{R}_0}{\partial \beta}\frac{\beta}{\mathcal{R}_0} = \frac{(\nu+\alpha+\mu)}{\gamma(\alpha+\mu)+\mu(\nu+\alpha+\mu)} \times \frac{\beta\big(\gamma(\alpha+\mu)+\mu(\nu+\alpha+\mu)\big)}{\beta(\nu+\alpha+\mu)} = 1.$$

The positive sign indicates a direct correlation between β and $\mathcal{R}_0$. A unit increase in β will provide a unit rise in $\mathcal{R}_0$.

Similarly, taking the derivative with respect to the other parameters yields.

$$\begin{aligned}
\Gamma_{\mu}^{\mathcal{R}_0} &= \frac{\partial \mathcal{R}_0}{\partial \mu}\frac{\mu}{\mathcal{R}_0} = -\frac{\mu\left((\nu+\alpha+\mu)^2+\gamma\nu\right)}{\left[\gamma(\alpha+\mu)+\mu(\nu+\alpha+\mu)\right]\left(\nu+\alpha+\mu\right)} < 0,\\
\Gamma_{\nu}^{\mathcal{R}_0} &= \frac{\partial \mathcal{R}_0}{\partial \nu}\frac{\nu}{\mathcal{R}_0} = \frac{\gamma\nu(\alpha+\mu)}{\left[\gamma(\alpha+\mu)+\mu(\nu+\alpha+\mu)\right]\left(\nu+\alpha+\mu\right)} > 0,\\
\Gamma_{\alpha}^{\mathcal{R}_0} &= \frac{\partial \mathcal{R}_0}{\partial \alpha}\frac{\alpha}{\mathcal{R}_0} = -\frac{\nu\gamma\alpha}{\left[\gamma(\alpha+\mu)+\mu(\nu+\alpha+\mu)\right]\left(\nu+\alpha+\mu\right)} < 0,\\
\Gamma_{\gamma}^{\mathcal{R}_0} &= \frac{\partial \mathcal{R}_0}{\partial \gamma}\frac{\gamma}{\mathcal{R}_0} = -\frac{\gamma(\alpha+\mu)}{\gamma(\gamma+\mu)+\mu(\nu+\alpha+\mu)} < 0.
\end{aligned} \tag{3.5}$$

Since the sensitivity index with respect to ν is positive, an increase in ν leads to an increase in the basic reproduction number $\mathcal{R}_0$. In contrast, the sensitivity indices corresponding to α, μ, and γ are negative, indicating that increasing any of these parameters results in a reduction of $\mathcal{R}_0$, while decreasing them leads to an increase in the basic reproduction number.

Using the parameter values $\mu = 0.0129$, $\nu = 0.010747$, $\alpha = 0.0737$, and $\gamma = 0.061735$, the corresponding sensitivity indices of the basic reproduction number $\mathcal{R}_0$ were computed to illustrate the individual influence of each parameter on the transmission potential of the disease.

Table 1. Parameters and sensitivity index

Parameter	**Sensitivity Index**
β	+1
μ	−0.2035
ν	+0.08939
α	−0.0760
γ	−0.9118

Figure 2a presents the bar plot of the calculated sensitivity indices, illustrating the magnitude and direction of influence for each parameter within the formulation of the basic reproduction number. The results show that the sensitivity indices associated with the transmission rate β and the progression parameter ν are positive, whereas the indices corresponding to α, μ, and γ are negative. This indicates that increasing either β or ν leads to an increase in the basic reproduction number $\mathcal{R}_0$, while increasing α, μ, or γ contributes to a decrease in $\mathcal{R}_0$.

The 3D plots illustrate how the basic reproduction number $\mathcal{R}_0$ varies with key epidemiological parameters. In Figure 2b, $\mathcal{R}_0$ increases with the transmission rate β and decreases with the recovery rate γ, highlighting the balance between infection and recovery. In Figure 2c, $\mathcal{R}_0$ increases with β but decreases with the natural death rate μ, as higher mortality reduces the infectious period. Panel Figure 2d shows the combined influence of the progression rate ν and the immunity loss rate α, where their interaction affects the overall transmission dynamics. Finally,Figure 2e demonstrates that $\mathcal{R}_0$ increases with both ν and β, indicating that faster progression to infectiousness and higher transmission jointly amplify disease spread.

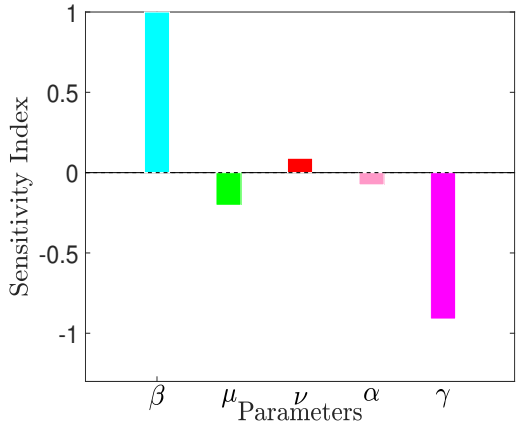

(a) Sensitivity index bar.

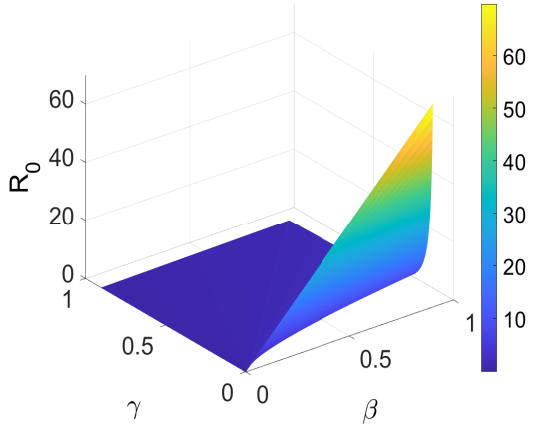

(b) The relation ship among $\mathcal{R}_0$, β, and γ.

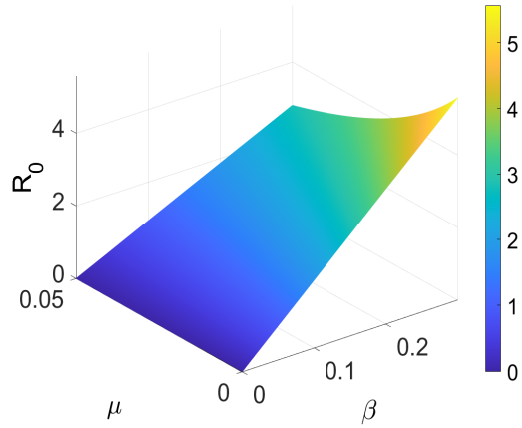

(c) The relationship among $\mathcal{R}_0$, β, and μ.

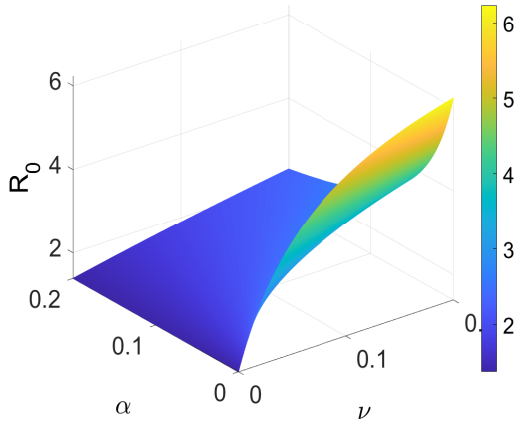

(d) The relationship among $\mathcal{R}_0$, ν, and α.

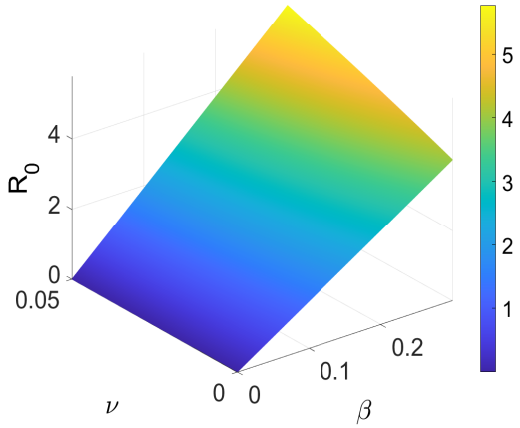

(e) The relationship among $\mathcal{R}_0$, β,and ν.

Figure 2. Parameter sensitivity and impact on $\mathcal{R}_0$.

Figure 3 (a-f) presents the contour map illustrating the different levels of the basic reproduction num-

ber $\mathcal{R}_0$ as a function of the main epidemiological parameters. The contour lines connect regions where $\mathcal{R}_0$ remains constant, while the variation in colors ranging from lighter to darker shades reflects the intensity of the epidemic risk. Darker regions indicate higher values of $\mathcal{R}_0$, associated with increased transmission, whereas lighter areas correspond to lower levels of the reproduction number. This representation effectively complements the three-dimensional surface plot by providing a clearer reading of the critical parameter thresholds that determine whether the infection can be controlled or is likely to continue spreading further.

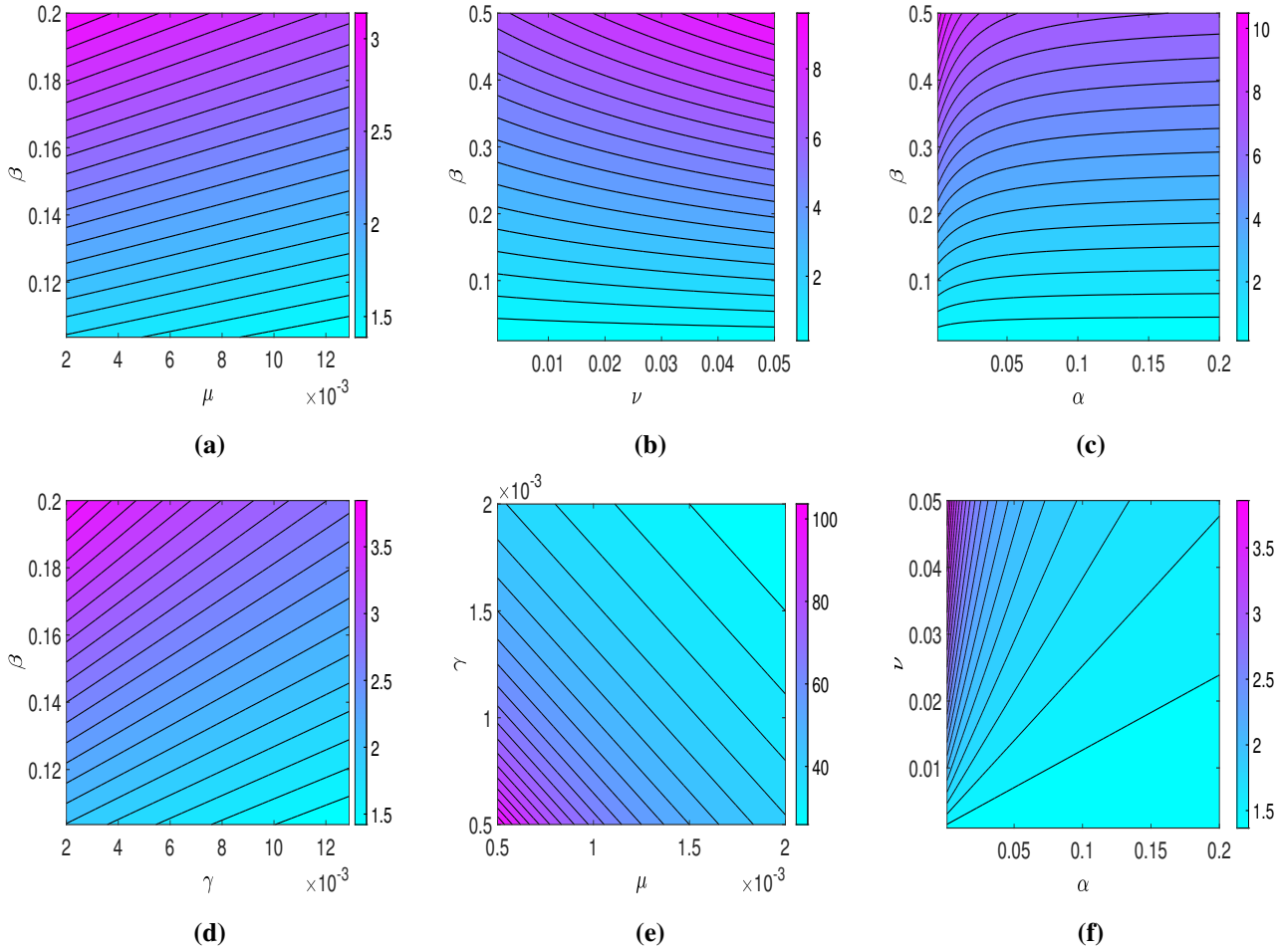

Figure 3. Contour plots of the basic reproduction number $\mathcal{R}_0$ as a function of key epidemiological parameter pairs: (a) (β, μ), (b) (β, ν), (c) (β, α), (d) (β, γ), (e) (γ, μ), (f) (ν, α).

3.4. The endemic equilibrium point E^*

After analyzing the disease-free case, we now turn to the situation in which tuberculosis (TB) infection persists within the population. In what follows, we consider system (2.1)–(2.2) in the absence of the time delay, which allows us to determine the equilibrium states in their algebraic form. We define the endemic equilibrium of the delay-free system as

$$E^* = (S_1^*, I_1^*, R^*, S_2^*, I_2^*),$$

which represents a steady state in which the infection persists over time. To determine this equilibrium, we set all time derivatives in the system equal to zero, thereby converting the differential equations into a system of algebraic equations that the equilibrium point must satisfy. These equations can be written in the following form:

$$\mu(N - S_1) - \beta\frac{S_1}{N}\left[I_1 + \phi I_2\right] = 0 \tag{3.6a}$$

$$\beta\frac{S_1}{N}\left[I_1 + \phi I_2\right] - \gamma I_1 + \nu R - \mu I_1 = 0 \tag{3.6b}$$

$$\gamma I_1 + \gamma I_2 - (\nu + \alpha + \mu)R = 0 \tag{3.6c}$$

$$\alpha R - \mu S_2 - \beta\frac{S_2}{N}\left[I_1 + \phi I_2\right] = 0 \tag{3.6d}$$

$$\beta\frac{S_2}{N}\left[I_1 + \phi I_2\right] - (\mu + \gamma)I_2 = 0 \tag{3.6e}$$

Obviously from equation (3.6a), (3.6c) and (3.6d) we obtain that

$$S_1^* = \frac{\mu N^2}{\mu N + \beta\left[I_1^* + \phi I_2^*\right]},\ R^* = \frac{\gamma(I_1^* + I_2^*)}{\nu + \alpha + \mu},\ S_2^* = \frac{\alpha\gamma N\left[I_1^* + \phi I_2^*\right]}{(\nu + \alpha + \mu)(\mu N + \beta\left[I_1^* + \phi I_2^*\right])}. \tag{3.7}$$

By substituting the given values into equations (3.6b), we obtain

$$f(I_1, I_2) = \frac{\beta\mu N\left[I_1 + \phi I_2\right]}{\mu N + \beta\left[I_1 + \phi I_2\right]} - (\gamma + \mu)I_1 + \frac{\nu\gamma\left[I_1 + \phi I_2\right]}{\nu + \alpha + \mu} = 0, \tag{3.8}$$

we have

$$\frac{\partial f(0,0)}{\partial I_1} = \beta - (\gamma + \mu) + \frac{\nu\gamma}{(\nu + \alpha + \mu)} = \frac{(\mathcal{R}_0 - 1)}{(\nu + \alpha + \mu)}, \frac{\partial f(0,0)}{\partial I_2} = \beta\phi + \frac{\nu\alpha\phi}{(\nu + \alpha + \mu)}.$$

We can conclude that if $\mathcal{R}_0 > 1$ then

$$\frac{\partial f(0,0)}{\partial I_1} > 0, \qquad \frac{\partial f(0,0)}{\partial I_2} > 0,$$

which implies that $f(I_1, I_2) > f(0,0) = 0$ if $\mathcal{R}_0 > 1$. This allows us to state the following theorem

Theorem 2. *For system* (2.1)–(2.2) *there always exists a disease-free equilibrium point* $E^0 = (N, 0, 0, 0, 0)$*; and if* $\mathcal{R}_0 > 1$*, then there also exists an endemic equilibrium point* $E^* = (S_1^*, I_1^*, R^*, S_2^*, I_2^*)$.

4. Stability analysis and Hopf bifurcation

In this section, we investigate the qualitative dynamical behavior of system (2.1)–(2.2) by examining the stability properties of its equilibrium points. The model admits two biologically meaningful steady states: the disease-free equilibrium E^0, which represents a population with no infection, and the endemic equilibrium E^*, which reflects the persistent presence of the disease when transmission is sustained. Our analysis aims to determine the local stability of these equilibria and to identify the conditions under which the infection either dies out or remains endemic within the community. To

achieve this, we linearize the system around each equilibrium and derive the corresponding characteristic equations, which form the basis for the stability analysis. Furthermore, studying how the roots of these equations vary with respect to the system parameters particularly the time delay allows us to detect the occurrence of a Hopf bifurcation, where the delay may lead to a loss of stability and the emergence of oscillatory dynamics in the disease transmission.

4.1. Local stability of the disease-free equilibrium E^0

In this part, we analyze the local stability of the disease-free equilibrium point E_0 of system (2.1)–(2.2). To carry out this analysis, we introduce suitable perturbation variables that represent small deviations from the equilibrium. Using these variables, we derive the linearized form of system (2.1)–(2.2) around the disease-free equilibrium E_0. The resulting linear system can be written as follows

$$\begin{cases} \dfrac{d\bar{S}_1(t)}{dt} = \mu\bar{S}_1(t) - \beta\bar{I}_1(t-\tau) - \phi\beta\bar{I}_2(t-\tau), \\ \dfrac{d\bar{I}_1(t)}{dt} = \beta\bar{I}_1(t-\tau) - (\gamma+\mu)\bar{I}_1(t) + \nu\bar{R}(t) + \phi\beta\bar{I}_2(t-\tau), \\ \dfrac{d\bar{R}(t)}{dt} = \gamma\bar{I}_1(t) - (\nu+\alpha+\mu)\bar{R}(t) + \gamma\bar{I}_2(t), \\ \dfrac{d\bar{S}_2(t)}{dt} = \alpha\bar{R}(t) - \mu\bar{S}_2(t), \\ \dfrac{d\bar{I}_2(t)}{dt} = -(\mu+\gamma)\bar{I}_2(t). \end{cases} \tag{4.1}$$

Next, by assuming solutions of exponential form for the perturbation variables and inserting them into the linearized system (4.1), we obtain the characteristic equation associated with the disease-free equilibrium E_0, given by

$$\begin{vmatrix} \lambda+\mu & \beta e^{-\lambda\tau} & 0 & 0 & \phi\beta e^{-\lambda\tau} \\ 0 & \lambda+(\gamma+\mu)-\beta e^{-\lambda\tau} & -\nu & 0 & -\phi\beta e^{-\lambda\tau} \\ 0 & -\gamma & \lambda+(\nu+\alpha+\mu) & 0 & -\gamma \\ 0 & 0 & -\alpha & \lambda+\mu & 0 \\ 0 & 0 & 0 & 0 & \lambda+(\mu+\gamma) \end{vmatrix} = 0. \tag{4.2}$$

Thus

$$(\lambda+\mu)^2(\lambda+\mu+\gamma)\left[(\lambda-\beta e^{-\lambda\tau}+(\mu+\gamma))(\lambda+\nu+\alpha+\mu)-\nu\gamma\right] = 0. \tag{4.3}$$

The analysis will be carried out by considering two separate cases. Under the condition $\tau = 0$, equation (4.3) becomes

$$(\lambda+\mu)^2(\lambda+\mu+\gamma)\left[(\lambda-\beta+(\mu+\gamma))(\lambda+\nu+\alpha+\mu)-\nu\gamma\right] = 0. \tag{4.4}$$

Clearly, from the matrix, we have three eigenvalues, which are

$$-\mu, -\mu, \text{ and } -(\mu+\gamma),$$

and the other eigenvalues are obtained from the following quadratic equation

$$\lambda^2 + \frac{1}{(\nu+\alpha+\mu)}\big((1-\mathcal{R}_0) + (\nu+\alpha+\mu)^2 + \nu\gamma\big)\lambda + (1-\mathcal{R}_0) = 0. \tag{4.5}$$

Applying the Routh-Hurwitz criterion [29] for a second-degree polynomial, the roots of this quadratic equation have negative real parts if and only if the coefficient of λ and the constant term are both positive. This condition is satisfied when $\mathcal{R}_0 < 1$, ensuring that all eigenvalues have negative real parts. Consequently, the disease-free equilibrium (DFE) point is locally asymptotically stable if $\mathcal{R}_0 < 1$ for $\tau = 0$.

Next, we move to treat the case when $\tau > 0$. In this case, the roots of equation (4.3) are given by

$$\lambda_1 = \lambda_2 = -\mu, \qquad \lambda_3 = -(\mu+\gamma),$$

and the remaining roots are determined by the solutions of the following equation:

$$F(\lambda) = \left(\lambda - \beta e^{-\lambda\tau} + (\mu+\gamma)\right)(\lambda+\nu+\alpha+\mu) - \nu\gamma = 0. \tag{4.6}$$

Note that, for $\lambda \in \mathbb{R}$, it is readily seen that

$$\lim_{\lambda\to+\infty} F(\lambda) = +\infty.$$

Furthermore, using $\mathcal{R}_0$, we obtain

$$F(0) = \big(-\beta + (\mu+\gamma)\big)(\nu+\alpha+\mu) - \nu\gamma = (1-\mathcal{R}_0).$$

If $\mathcal{R}_0 > 1$, then $(1-\mathcal{R}_0) < 0$ and consequently $F(0) < 0$. Hence, by the intermediate value theorem [30], it follows that equation $F(\lambda) = 0$ admits a positive real root whenever $\mathcal{R}_0 > 1$.

Now, assume $\mathcal{R}_0 < 1$. Let λ be any root of the characteristic equation (4.6) and suppose $\mathrm{Re}(\lambda) \geq 0$. Write

$$F(\lambda) = \left(\lambda - \beta e^{-\lambda\tau} + (\mu+\gamma)\right)(\lambda+\nu+\alpha+\mu) - \nu\gamma, \tag{4.7}$$

so that, taking real parts,

$$\mathrm{Re}(F(\lambda)) = \big(\mathrm{Re}(\lambda) - \beta e^{-\mathrm{Re}(\lambda)\tau}\cos(\mathrm{Im}(\lambda)\tau) + (\mu+\gamma)\big)\big(\mathrm{Re}(\lambda)+\nu+\alpha+\mu\big) - \nu\gamma.$$

Since $e^{-\mathrm{Re}(\lambda)\tau} \leq 1$ and $\cos(\mathrm{Im}(\lambda)\tau) \leq 1$, we have

$$\mathrm{Re}(\lambda) - \beta e^{-\mathrm{Re}(\lambda)\tau}\cos(\mathrm{Im}(\lambda)\tau) + (\mu+\gamma) \geq \mathrm{Re}(\lambda) + (\mu+\gamma) - \beta \geq (\mu+\gamma) - \beta,$$

and

$$\mathrm{Re}(\lambda) + (\nu+\alpha+\mu) \geq (\nu+\alpha+\mu).$$

Thus,

$$\mathrm{Re}(F(\lambda)) \geq \big((\mu+\gamma)-\beta\big)(\nu+\alpha+\mu) - \nu\gamma = (1-\mathcal{R}_0) > 0.$$

This is a contradiction because λ was assumed to be a root of the characteristic equation, so $F(\lambda) = 0$, and thus $\mathrm{Re}\left(F(\lambda)\right) = 0$. Therefore, no root λ can satisfy $\mathrm{Re}(\lambda) \geq 0$. Hence, all roots must have negative real part when $\mathcal{R}_0 < 1$.

Theorem 3. *The disease-free equilibrium E^0 is locally asymptotically stable if $\mathcal{R}_0 < 1$ and unstable if $\mathcal{R}_0 > 1$.*

4.2. Local stability of the endemic equilibrium point E^*

In this section, we investigate the local stability and the possible occurrence of a Hopf bifurcation around the endemic equilibrium E^*. To this end, we linearize system (2.1)–(2.2) in a neighborhood of this equilibrium. Introducing the perturbation variables

$$\bar{S}_1(t) = S_1(t) - S_1^*, \qquad \bar{I}_1(t) = I_1(t) - I_1^*, \qquad \bar{R}(t) = R(t) - R^*,$$
$$\bar{S}_2(t) = S_2(t) - S_2^*, \qquad \bar{I}_2(t) = I_2(t) - I_2^*,$$

we obtain the following linearized system:

$$\begin{cases} \dfrac{d\tilde{S}_1(t)}{dt} = a_{11}\tilde{S}_1(t) + a_{12}\tilde{S}_1(t-\tau) + a_{13}\tilde{I}_1(t-\tau) + a_{14}\tilde{I}_2(t-\tau), \\ \dfrac{d\tilde{I}_1(t)}{dt} = a_{21}\tilde{S}_1(t-\tau) + a_{22}\tilde{I}_1(t-\tau) + a_{23}\tilde{I}_1(t) + a_{24}\tilde{R}(t) + a_{25}\tilde{I}_2(t-\tau), \\ \dfrac{d\tilde{R}(t)}{dt} = a_{31}\tilde{I}_1(t) + a_{32}\tilde{R}(t) + a_{33}\tilde{I}_2(t), \\ \dfrac{d\tilde{S}_2(t)}{dt} = a_{41}\tilde{I}_1(t) + a_{42}\tilde{R}(t) + a_{43}\tilde{S}_2(t) + a_{44}\tilde{I}_2(t), \\ \dfrac{d\tilde{I}_2(t)}{dt} = a_{51}\tilde{I}_1(t) + a_{52}\tilde{S}_2(t) + a_{53}\tilde{I}_2(t), \end{cases} \tag{4.8}$$

where

$$a_{11} = -\mu, \ \ a_{12} = -\frac{\beta[I_1^* + \phi I_2^*]}{N}, \ \ a_{13} = -\frac{\beta_1 S_1^*}{N}, \ \ a_{14} = -\frac{\phi\beta_1 S_1^*}{N}, \ \ a_{21} = \frac{\beta[I_1^* + \phi I_2^*]}{N},$$
$$a_{22} = \frac{\beta_1 S_1^*}{N}, \ \ a_{23} = -(\mu + \gamma), \ \ a_{24} = \nu, \ \ a_{25} = \frac{\phi\beta_1 S_1^*}{N}, \ \ a_{31} = \gamma, \ \ a_{32} = -(\mu + \alpha + \nu),$$
$$a_{33} = \gamma, \ \ a_{41} = -\frac{\beta_1 S_2^*}{N}, \ \ a_{42} = \alpha, \ \ a_{43} = -\mu - \frac{\beta[I_1^* + \phi I_2^*]}{N}, \ \ a_{44} = -\frac{\phi\beta_1 S_2^*}{N}, \ \ a_{51} = \frac{\beta S_2}{N},$$
$$a_{52} = \frac{\beta[I_1^* + \phi I_2^*]}{N}, \ \ a_{53} = \frac{\phi\beta_1 S_2^*}{N} - (\gamma + \mu).$$

Furthermore, by considering the exponential solutions $\tilde{S}(t) = x_1 e^{\lambda t}, \tilde{I}_1(t) = x_2 e^{\lambda t}, \bar{R}(t) = x_3 e^{\lambda t}, \tilde{S}_1(t) = x_4 e^{\lambda t}, \tilde{I}_2(t) = x_5 e^{\lambda t}$, we substutite them into the linear system (4.8). This allows us to write the characteristic equation at the equilibrium point E^* as follows

$$\begin{vmatrix} a_{11} + a_{12}e^{-\lambda\tau} - \lambda & a_{13}e^{-\lambda\tau} & 0 & 0 & a_{14}e^{-\lambda\tau} \\ a_{21}e^{-\lambda\tau} & a_{22}e^{-\lambda\tau} + a_{23} - \lambda & a_{24} & 0 & a_{25}e^{-\lambda\tau} \\ 0 & a_{31} & a_{32} - \lambda & 0 & a_{33} \\ 0 & a_{41} & a_{42} & a_{43} - \lambda & a_{44} \\ 0 & a_{51} & 0 & a_{52} & a_{53} - \lambda \end{vmatrix} = 0. \tag{4.9}$$

Thus, we could get

$$(\lambda^5 + P_4\lambda^4 + P_3\lambda^3 + P_2\lambda^2 + P_1\lambda + P_0) + (Q_4\lambda^4 + Q_3\lambda^3 + Q_2\lambda^2 + Q_1\lambda + Q_0)e^{-\lambda\tau} + (M_3\lambda^3 + M_2\lambda^2 + M_1\lambda + M_0)e^{-2\lambda\tau} = 0 \quad (4.10)$$

where

$$\begin{aligned}
P_4 =& -(a_{11} + a_{23} + a_{32} + a_{43} + a_{53}),\\
P_3 =& a_{11}(a_{23} + a_{32} + a_{43} + a_{53}) + a_{23}(a_{32} + a_{43} + a_{53}) + a_{43}a_{53} + a_{32}(a_{43} + a_{53}) - a_{52}a_{44} - a_{24}a_{31},\\
P_2 =& -a_{11}(a_{32}a_{23} - a_{52}a_{44} - a_{24}a_{31}) - a_{32}a_{43}a_{53} - a_{23}a_{43}a_{53} - a_{33}a_{42}a_{52} + a_{32}a_{52}a_{44} + a_{23}a_{52}a_{44}\\
&- a_{24}a_{33}a_{51} - (a_{43} + a_{53})(a_{12}a_{32} + a_{23}a_{32} + a_{24}a_{31} + a_{11}a_{23}),\\
P_1 =& -a_{11}(a_{32}a_{43}a_{53} + a_{23}a_{43}a_{53} - a_{32}a_{52}a_{44} - a_{23}a_{52}a_{44} + a_{24}a_{33}a_{51}) + a_{24}a_{31}(a_{43} + a_{53})\\
&- a_{23}a_{32}(a_{52}a_{44} - a_{43}a_{53}) - a_{24}a_{33}(a_{41}a_{52} - a_{51}a_{43}) - a_{31}a_{24}(a_{43}a_{53} - a_{52}a_{44}) + a_{23}a_{33}a_{42}a_{52}\\
&+ a_{12}a_{33}a_{42}a_{42},\\
P_0 =& a_{11}a_{23}(a_{32}a_{43}a_{53} - a_{32}a_{52}a_{44} + a_{33}a_{42}a_{52}) + a_{11}a_{31}(a_{42}a_{52}a_{44} - a_{24}a_{43}a_{53}) + a_{24}a_{11}a_{33}a_{51}a_{43}\\
&- a_{42}a_{11}a_{33}a_{41}a_{52},\\
Q_4 =& -a_{22} - a_{12}, \quad Q_3 = a_{12}(a_{43} + a_{53} + a_{32} + a_{23}) + a_{22}(a_{32} + a_{43} + a_{53} + a_{11}) - a_{25}a_{51},\\
Q_2 =& -a_{43}a_{53}(a_{12} + a_{22}) - (a_{43} + a_{53})(a_{12}a_{32} + a_{22}a_{32} + a_{11}a_{22} + a_{12}a_{23}) - a_{32}(a_{11}a_{22} + a_{12}a_{23})\\
&+ a_{12}(a_{32}a_{43} + a_{32}a_{53} + a_{43}a_{53} - a_{52}a_{44}) + a_{23}(a_{32}a_{43} + a_{32}a_{53} + a_{43}a_{53} - a_{52}a_{44}) + a_{24}a_{12}a_{31}\\
&+ a_{52}a_{44}(a_{12} + a_{22}) - a_{25}(a_{41}a_{52} - a_{11}a_{51}),\\
Q_1 =& a_{43}a_{53}(a_{22}a_{32} + a_{11}a_{22} + a_{12}a_{23} + a_{12}a_{32}) + (a_{43} + a_{53})(a_{11}a_{22}a_{32} + a_{12}a_{23}a_{32} + a_{24}a_{12}a_{31})\\
&- a_{52}a_{44}(a_{12}a_{32} + a_{22}a_{32} + a_{11}a_{22} + a_{12}a_{22} + a_{12}a_{23}) + a_{42}a_{52}(a_{12}a_{33} + a_{22}a_{33} - a_{25}a_{31})\\
&- a_{25}a_{11}(a_{51}a_{43} - a_{41}a_{52} + a_{32}a_{51}) - a_{25}a_{32}(a_{51}a_{43} - a_{41}a_{52}) + a_{25}a_{51}(a_{43} + a_{51})\\
&+ a_{24}a_{12}a_{33}a_{51},\\
Q_0 =& -a_{11}a_{22}(a_{43}a_{53} - a_{32}a_{52}a_{44} + a_{33}a_{42}a_{52}) - a_{12}a_{23}a_{52}(a_{33}a_{42} - a_{32}a_{44} - a_{12}a_{23}a_{32}a_{43}a_{53}\\
&+ a_{24}a_{12}(a_{33}a_{51}a_{43} - a_{31}(a_{43} + a_{52})) + a_{25}a_{11}(a_{31}a_{42}a_{53} - a_{32}a_{41}a_{52} + a_{32}a_{51}a_{43})\\
&+ a_{24}a_{12}a_{31}(a_{52}a_{44} - a_{43}a_{53}),\\
M_3 =& a_{12}a_{22} - a_{13}a_{21},\\
M_2 =& -(a_{12}a_{22} - a_{13}a_{21})(a_{43} + a_{53}) - a_{12}a_{22}a_{32} + a_{25}a_{12}a_{51} + a_{13}a_{21}a_{32} - a_{14}a_{21}a_{51},\\
M_1 =& a_{12}a_{22}a_{43}a_{53} - (a_{43} + a_{53})(a_{13}a_{21}a_{32} - a_{12}a_{22}a_{32}) - a_{25}a_{12}(a_{51}a_{43} + a_{32}a_{51} - a_{41}a_{52}),\\
&- a_{13}a_{21}(a_{43}a_{53} - a_{52}a_{44}) + a_{14}a_{21}(a_{41}a_{52} + a_{51}a_{43} + a_{32}a_{51}),\\
M_0 =& -a_{12}a_{22}a_{33}a_{42}a_{52} - a_{25}a_{12}a_{32}(a_{41}a_{52} - a_{51}a_{43}) + a_{13}a_{21}(a_{32}a_{43}a_{53} - a_{32}a_{52}a_{44} + a_{33}a_{42}a_{52})\\
&- a_{14}a_{21}(a_{31}a_{42}a_{52} - a_{32}a_{41} + a_{23}a_{51}a_{43}) - a_{12}a_{22}(a_{32}a_{43}a_{53} - a_{32}a_{53}a_{44}) + a_{25}a_{12}a_{31}a_{42}a_{52}.
\end{aligned}$$

4.2.1. Analysis of the system without delay ($\tau = 0$)

We begin our analysis with the case where the delay is absent in order to understand the behaviour of the solutions in this simplified setting. To do so, we set $\tau = 0$ in system (4.10), which reduces the model to an ordinary differential framework. Substituting $\tau = 0$ into the linearized system allows us to derive the corresponding characteristic equation for the undelayed case. In this situation, the characteristic equation takes the following form:

$$\lambda^5 + B_4\lambda^4 + N + B_3\lambda^3 + B_2\lambda^2 + B_1\lambda + B_0, \quad (4.11)$$

where

$$B_4 = P_4 + Q_4, \;\; B_3 = P_3 + Q_3 + M_3, \;\; B_2 = P_2 + Q_2 + M_2,$$
$$B_1 = P_1 + Q_1 + M_1, \;\; B_0 = P_0 + Q_1 + M_0.$$

By applying the Routh–Hurwitz criterion, the stability of the equilibrium can be assessed directly from the coefficients of the characteristic equation (4.11). According to this criterion, all roots of the characteristic equation have negative real parts, and therefore the equilibrium is locally asymptotically stable if and only if a specific sequence of positivity conditions involving the determinants constructed from the polynomial coefficients is satisfied. In the present case, where the characteristic equation is of fifth degree, the necessary and sufficient conditions for stability are given by the positivity of the determinants associated with the Routh–Hurwitz matrix corresponding to a fifth–degree polynomial.

$$B_4 > 0, \quad \begin{vmatrix} B_1 & 1 \\ B_3 & B_2 \end{vmatrix} > 0, \quad \begin{vmatrix} B_4 & 1 & 0 \\ B_2 & B_3 & B_4 \\ B_0 & B_1 & B_1 \end{vmatrix} > 0, \quad \begin{vmatrix} B_4 & 1 & 0 & 0 \\ B_2 & B_3 & B_4 & 1 \\ B_0 & B_1 & B_1 & 0 \\ 0 & 0 & B_0 & B_1 \end{vmatrix} > 0. \tag{4.12}$$

Theorem 4. *For $\tau = 0$, the endemic equilibrium E^* is locally asymptotically stable if and only if the Routh–Hurwitz stability conditions given in* (4.12) *are satisfied.*

4.2.2. Analysis of the system with delay ($\tau > 0$)

In the presence of a delay, the characteristic equation of the linearized system contains exponential terms that may generate purely imaginary roots and lead to a Hopf bifurcation. To simplify the analysis, and before proceeding further, we multiply both sides of equation (4.13) by the exponential expression $e^{\lambda\tau_1}$, which yields a more convenient form for studying the location of the characteristic roots. After this step, we obtain a characteristic equation of the following form

$$(Q_4\lambda^4 + Q_3\lambda^3 + Q_2\lambda^2 + Q_1\lambda + Q_0) + (\lambda^5 + P_4\lambda^4 + P_3\lambda^3 + P_2\lambda^2 + P_1\lambda + P_0)e^{\lambda\tau} + (M_3\lambda^3 + M_2\lambda^2 + M_1\lambda + M_0)e^{-\lambda\tau} = 0 \tag{4.13}$$

This new expression allows us to separate the real and imaginary parts of the roots and provides the basis for the stability analysis and for determining the critical values of the delay.

Now, suppose that previous equation has a pure imaginary root $\lambda = iw$ with $w > 0$. Then, by inserting it into (4.13), and by taking its real and imaginary parts, we could get

$$\begin{cases} -Q_4w^4 + Q_2w^2 - Q_0 = \big(P_4w^4 - (P_2 + M_2)w^2 + P_0 + M_0\big)\cos(w\tau) + \big(-w^5 + (P_3 - M_3)w^3 + (M_1 - P_1)w\big)\sin(w\tau), \\ -Q_3w^3 - Q_1w = \big(w^5 - (P_3 + M_3)w^3 + (P_1 + M_1)w\big)\cos(w\tau) + \big(P_4w^4 + (M_2 - P_2)w^2 + (P_0 - M_0)\big)\sin(w\tau). \end{cases}$$

Furthermore, from the previous system, we can obtain

$$\begin{cases} \sin(w\tau) = \dfrac{\eta_9w^9 + \eta_7w^7 + \eta_5w^5 + \eta_3w^3 + \eta_1w}{-w^{10} + \xi_8w^8 + \xi_6w^6 + \xi_4w^4 + \xi_2w^2 + \xi_0}, \\ \cos(w\tau) = \dfrac{\zeta_8w^8 + \zeta_6w^6 + \zeta_4w^4 + \zeta_2w^2 + \zeta_0}{-w^{10} + \xi_8w^8 + \xi_6w^6 + \xi_4w^4 + \xi_2w^2 + \xi_0}, \end{cases} \tag{4.14}$$

where

$$\begin{aligned}
&\eta_9 = -Q_4, \quad \eta_7 = Q_4(P_3 + M_3) + Q_2 + Q_3P_4,\\
&\eta_5 = -Q_4(P_1 + M_1) - Q_2(P_3 + M_3) - Q_0 - Q_3(P_2 + M_2) + Q_1P_4,\\
&\eta_3 = Q_0(P_3 + M_3) + Q_2(P_1 + M_1) + Q_3(P_0 + M_0) - Q_1(P_2 + M_2),\\
&\eta_1 = -Q_0(P_1 + M_1) + Q_1(P_0 + M_0), \quad \xi_8 = (P_3 + M_3) + (P_4 - M_3) - P_4^2,\\
&\xi_6 = -(P_1 + M_1) - (P_3 - M_3)(P_3 + M_3) + (M_1 - P_1) + 2P_4P_2,\\
&\xi_4 = (P_3 - P_3)(P_1 + M_1) - (M_1 - P_1)(P_3 + M_3) + (M_2 - P_2)(P_2 + M_3) - 2P_0P_4,\\
&\xi_2 = (M_1 - P_1)(P_1 + M_1) - (M_2 - P_2)(P_0 + M_0) + (P_0 - M_0)(P_2 + M_2),\\
&\xi_0 = -(P_0 - M_0)(P_0 + M_0), \quad \zeta_8 = Q_3, \quad \zeta_6 = -Q_2P_4 - Q_3(P_3 - M_3) + Q_1,\\
&\zeta_4 = Q_4P_4 - Q_2(M_2 - P_2) + Q_0P_4 - Q_3P_4 - Q_3(M_1 - P_1) - Q_1(P_3 - M_3),\\
&\zeta_2 = Q_4(M_2 - P_2) - Q_2(P_0 - M_0) + Q_0(M_2 - P_2) - Q_1(M_1 - P_1),\\
&\zeta_0 = (Q_4 + Q_0)(P_0 - M_0).
\end{aligned} \tag{4.15}$$

After that, by squaring equations of system (4.14), and combining them, we get

$$w^{20} + k_{18}w^{18} + k_{16}w^{16} + k_{14}w^{14} + k_{12}w^{12} + k_{10}w^{10} + k_8w^8 + k_6w^6 + k_4w^4 + k_2w^2 + k_0, \tag{4.16}$$

where

$$\begin{aligned}
&k_{18} = -(2\xi_8 - \eta_9^2), \quad k_{16} = \xi_8^2 - 2\xi_6 - 2\eta_9\eta_7 - 2\zeta_8\zeta_6 - \zeta_8^2,\\
&k_{14} = 2\zeta_8\zeta_6 - 2\xi_4 - \eta_7^2 - 2\eta_9\eta_5,\\
&k_{12} = \xi_6^2 + 2\xi_8\xi_4 - 2\xi_2 - 2\eta_9\eta_3 - 2\eta_7\eta_5 - \zeta_6^2 - 2\zeta_8\zeta_4,\\
&k_{10} = 2\xi_8\xi_2 + 2\xi_6\xi_4 - 2\xi_0 - \eta_5^2 - 2\eta_9\eta_1 - 2\eta_7\eta_3 - 2\zeta_8\zeta_2 - 2\zeta_6\zeta_4,\\
&k_8 = \xi_4^2 + 2\xi_8\xi_0 + 2\xi_6\xi_2 - 2\eta_7\eta_1 - 2\eta_5\eta_3 - \zeta_4^2 - 2\zeta_8\zeta_0 - 2\zeta_6\zeta_2,\\
&k_6 = 2\xi_6\xi_0 + 2\xi_4\xi_2 - \eta_3^2 - 2\eta_5\eta_1 - 2\zeta_6\zeta_0 - 2\zeta_4\zeta_2,\\
&k_4 = \xi_2^2 + 2\zeta_4\xi_0 - 2\eta_5\eta_1 - \zeta_2^2 - 2\zeta_4\zeta_0,\\
&k_2 = -\eta_1 - 2\zeta_2\zeta_0, \quad k_0 = \xi_0^2 - \zeta_0^2.
\end{aligned} \tag{4.17}$$

At this point, by setting $z = w^2$, equation (4.16) can be expressed as follows

$$\ell(z) = w^{10} + k_{18}w^9 + k_{16}w^8 + k_{14}w^7 + k_{12}w^6 + k_{10}w^5 + k_8w^4 + k_6w^3 + k_4w^2 + k_2w + k_0 = 0. \tag{4.18}$$

Next, through the use of intermediate value theorem, if $k_0 < 0$, then equation (4.18) has a positive root z statisfying $w = \pm\sqrt{z}$.

Without loss of generality, we assume that equation $\ell(z) = 0$ has many positive real roots denoted by z_i, $i = 1, 2, \cdots 10$, which implies that equation (4.16) also has multiple real roots $w_i = \sqrt{z_i}$, $i = 1, 2, \cdots, 10$.

Next, we pass to establish the critical value of time delay τ_0. To do this, from first equation of system (2.1), it follows that

$$\tau_i^k = \frac{1}{w_i}\arccos\left(\frac{\zeta_8w_i^8 + \zeta_6w_i^6 + \zeta_4w_i^4 + \zeta_2w_i^2 + \zeta_0}{-w_i^{10} + \xi_8w_i^8 + \xi_6w_i^6 + \xi_4w_i^4 + \xi_2w_i^2 + \xi_0}\right) + \frac{2k\pi}{w_i}, \tag{4.19}$$

with $i = 1, 2, \cdots, 10,\ k = 1, 2\cdots$. Therefore, when $\tau = \tau_i^k$, $i = 1, 2, \cdots, 10$, with $\tau_0 = \min_{i=\overline{1,10}}\{\tau_i^0\}$ and $w_0 = w_{i_0}$, then equation (4.13) admits a pair of purely imaginary roots $\pm iw_i$.

For the bifurcation analysis, the time delay τ is chosen as the bifurcation parameter, and we will show that there exists at least one root with positive real part for $\tau > \tau_0$.

With help of implicit function theorem [31], and by differentiating equation (4.13), we obtain

$$\left(\frac{d\lambda}{d\tau}\right)^{-1} = \frac{\left(4Q_4\lambda^3+3Q_3\lambda^2+2Q_2\lambda+Q_1\right)+\left(5\lambda^4+4P_4\lambda^3+3P_3\lambda^2+2P_2\lambda+P_1\right)e^{\lambda\tau}+\left(3M_3\lambda^2+2M_2\lambda+M_1\right)e^{-\lambda\tau}}{-\lambda\left[\left(\lambda^5+P_4\lambda^4+P_3\lambda^3+P_2\lambda^2+P_1\lambda+P_0\right)e^{\lambda\tau}-\left(M_3\lambda^3+M_2\lambda^2+M_1\lambda+M_0\right)e^{-\lambda\tau}\right]} - \frac{\tau}{\lambda} \tag{4.20}$$

Moreover, if we replace λ with iw_0 and extract the real component from the preceding equation (4.20), we can get

$$\mathrm{Re}\left(\frac{d\lambda}{d\tau}\right)^{-1}_{\lambda=iw_0} = \frac{G(w_0)}{\psi_1^2+\psi_2^2}, \tag{4.21}$$

where

$$G(w_0) = h_{10}w_0^{10} + h_9w_0^9 + h_8w_0^8 + h_7w_0^7 + h_6w_0^6 + h_5w_0^5 + h_4w_0^4 + h_3w_0^3 + h_2w_0^2 + h_1w_0, \tag{4.22}$$

with

$$\begin{aligned}
h_{10} =& -5\sin^2 w_0\tau,\\
h_9 =& \ 4Q_4\sin w_0\tau - 5P_4\sin w_0\tau\cos w_0\tau + 4\cos w_0\tau\sin w_0\tau,\\
h_8 =& -4Q_4\cos w_0\tau\sin w_0\tau + 4P_4 - 5M_2\sin w_0\tau + 4P_4Q_4\cos w_0\tau - (5P_3+3M_2)\sin^2 w_0\tau,\\
h_7 =& -3Q_2\cos w_0\tau + 3Q_2P_4\sin w_0\tau + 3(P_3+M_2)\cos^2 w_0\tau + 7(M_2+5P_2)\sin^2 w_0\tau - 2Q_1\sin w_0\tau\\
&+ (4M_3 - 3P_3P_4 + 4M_2 - 2P_2 - 3M_2P_4 - 3M_3P_4)\sin w_0\tau\cos w_0\tau + 4Q_4(M_2+P_3)\sin w_0\tau,\\
h_6 =& -Q_2P_3\cos w_0\tau + 3Q_2M_3\cos w_0\tau + (2P_2 + 4M_2 - 2M_2P_4 - 2M_2)\sin w_0\tau\cos w_0\tau\\
&+ (3P_3^2 - P_3M_3 - 2P_4 + 3M_2P_3 - 3M_2M_3)\cos^2 w_0\tau + Q_4(M_2-P_2)\sin w_0\tau + 2M_2P_4\sin w_0\tau\\
&+ (4P_1+M_1)\sin^2 w_0\tau + (-2P_2P_4 + 5M_1 + 3P_3 - 3M_2P_3 - 6M_2^2)\sin^2 w_0\tau - 2Q_1P_4\cos w_0\tau\\
&+ 2M_2P_4\sin w_0\tau,\\
h_5 =& -3M_2^2 - 2P_2P_3\sin w_0\tau\cos w_0\tau + 3Q_2(P_2+M_2)\cos w_0\tau - Q_1\cos w_0\tau - 4Q_1(P_1+M_1)\sin w_0\tau\\
&+ (-4P_1 + P_1P_4 - 2M_2P_3 + 2M_2M_3 + M_1P_4 + 3P_3P_4 - 2P_2M_2 - P_1P_4 + 5P_0)\sin w_0\tau\cos w_0\tau\\
&- 2Q_1(P_3+M_2)\sin w_0\tau - 8M_1\sin w_0\tau\cos w_0\tau + 5M_0\cos w_0\tau + 3M_2(P_2-P_3)\sin^2 w_0\tau\\
&- P_4M_1\sin w_0\tau - 2M_2^2\sin^2 w_0\tau - (M_1+P_1)\cos^2 w_0\tau + P_2(3M_2 - 6P_3)\cos^2 w_0\tau,\\
h_4 =& -4Q_4(P_0+M_0)\cos w_0\tau + 3Q_2(P_1-M_1)\cos w_0\tau - Q_1(P_3+M_3)\cos w_0\tau - P_1P_3 - P_3M_1\\
&+ (2P_2P_3 - 2P_2M_2 + 2M_2^2)\sin w_0\tau\cos w_0\tau + (-3P_3P_1 - 4M_0 + P_1M_3 + M_1M_3)\cos^2 w_0\tau\\
&+ (4M_0 + 3P_3M_2 + 3P_3^2 + 2P_1M_2 + 4P_0 + 2M_2P_2 - 2M_2^2 - M_1M_2)\sin^2 w_0\tau\\
&- 4Q_4(P_0+M_0)\cos w_0\tau + 2Q_1(P_2-M_2)\sin w_0\tau + 3M_2P_1(\sin^2 w_0\tau - \cos^2 w_0\tau),\\
h_3 =& 3Q_2(P_0+M_0)\sin w_0\tau + M_1M_2 + M_1P_2 + Q_1(P_2+Q_2)\cos w_0\tau + P_1P_2 + P_1M_2\cos^2 w_0\tau\\
&+ (4Q_2 - 3P_3P_0 - 3P_3M_0 + 2M_2P_1 - M_2M_1)\sin w_0\tau\cos w_0\tau\\
&+ Q_1(P_4 + 2P_1 + 2M_1)\sin w_0\tau + (-3P_3P_2 + 3P_4M_2 - P_1M_2 + 2P_1M_2)\sin^2 w_0\tau,
\end{aligned}$$

$$
\begin{aligned}
h_2 &= Q_1(P_1 - M_1)\cos w_0\tau - 3P_3M_1 - 2(P_2 + M_2)(P_0 + M_0)\sin^2 w_0\tau + 4M_2P_0 \sin w_0\tau \\
&\quad + (P1^2 + M_1^2)\sin^2 w_0\tau + 2P_1M_1 \sin^2 w_0\tau + 2P_2(P_0 + M_0)\cos^2 w_0\tau - M_1^2 \cos^2 w_0\tau \\
&\quad + Q_1(M_0 + 2p_0)\cos w_0\tau - 3P_3P_1 \sin^2 w_0\tau + 2M_2M_0 \cos w_0\tau \sin w_0\tau, \\
h_1 &= Q_1(P_0 + M_0)\sin w_0\tau + (2P_1P_0 + 2P_1M_0 + M_1P_0 + M_1M_0 - 6P_3P_0)\cos w_0\tau \sin w_0\tau, \\
\psi_1 &= (P_4 \sin w_0\tau - \cos w_0\tau)w_0^5 + (M_3 - P_5)w_0 \cos w_0\tau + (P_2 + M_2)w_0^3 \cos w_0\tau \\
&\quad + (P_0 + M_0)w_0 \sin^2 w_0\tau + (P_2 - M_1)w_0^2 \cos^2 w_0\tau, \\
\psi_2 &= -w_0^6 \sin w_0\tau - P_4w_0^5 \cos w_0\tau - (P_3 + M_3)w_0^4 \sin w_0\tau + (P_2 - M_2)w_0^3 \sin w_0\tau \\
&\quad + (P_1 + M_1)w_0^2 \sin w_0\tau + (P_0 + M_0)w_0 \cos w_0\tau.
\end{aligned}
$$

Theorem 5. *For $\tau > 0$, if $k_0 < 0$ then there exists a critical value of delay time τ_0 such that the endemic equilibrium point E^* is locally asymptotically for $\tau < \tau_0$ and is unstable for $\tau > \tau_0$. Also, if $G(w_0) > 0$, Hopf-bifurcation is exhibited by the system at $\tau = \tau_0$.*

5. Numerical results and analysis

In this part of the study, four essential model parameters are identified by fitting the model to tuberculosis incidence data reported in the World Health Organization (WHO) Global TB Report [32] for the period 1990–2024 (see Table 2). These parameters are estimated so that the model accurately reflects the observed trends in the reported cases throughout these years. The remaining parameters are chosen based on reliable statistical information and empirical values commonly documented in previous epidemiological studies, ensuring consistency with established findings in the literature. In this study, the initial conditions were determined using updated demographic and epidemiological data for Algeria. The total population at the initial time was set to $N(0) = 25{,}407{,}615$, based on World Bank [33] estimates for the year 1990. The number of individuals in the first infectious class was taken as $I_1(0) = 11{,}607$, in accordance with the TB incidence reported for that year.

The initial treated population was computed using the treatment success relation

$$\text{Successful treatments} = \left(\frac{\text{Treatment Success Rate (\%)}}{100}\right) \times \text{New TB cases},$$

which yields $R(0) = 10{,}098$. Furthermore, the initial exposed population was set to $S_2(0) = 80{,}152$, while the second infectious class was initialized as $I_2(0) = 70{,}000$.

Since the model considers the susceptible population as the portion of the population not belonging to any other compartment, and given that the initial infection levels represent a very small proportion of the total population, the common assumption $S_1(0) = N(0)$ was adopted at the initial time.

These initial conditions were carefully selected to ensure internal consistency within the model and to support realistic numerical simulations of tuberculosis transmission in Algeria.

5.1. Model parameter fitting

To determine the parameter values ϕ, α, β, a nonlinear regression approach was employed to obtain the optimal set of values that enables the model to reproduce the observed trends of tuberculosis transmission. The estimation procedure relies on minimizing the discrepancy between the recorded

data and the solutions generated by the model. For this purpose, the objective function is defined as follows:

$$F = \sum_{i=1}^{n} \left(I_{1t_i}^{\text{data}} - I_{1t_i}^{\text{model}} \right)^2, \tag{5.1}$$

where $I_{1t_i}^{\text{data}}$ denotes the observed number of cases at time t_i, $I_{1t_i}^{\text{model}}$ represents the corresponding value predicted by the model, and n is the total number of available data points. Minimizing this function yields the optimal parameter values, ensuring that the model accurately reflects the real epidemiological behavior.

For clarity of presentation, all estimated parameter values are summarized in a separate table see Table 2. Furthermore, a graphical comparison between the real incidence data and the fitted model output is provided to assess the estimation quality and the model's ability to capture the temporal evolution of the disease (see Figure 4).

Table 2. Initial values and parameter settings of the model.

Parameter	**Algeria's Parameters**	**source**
$S_1(0)$	25,407,615	World Bank [33]
$I_1(0)$	11,607	[32]
$R(0)$	10,098	Calculated
$S_2(0)$	80,152	Assumed
$I_2(0)$	70,000	Assumed
β	0.52720 (dimensionless)	Fitted
μ	$1/77(year^{-1})$	World Bank [33]
γ	0.5 $(year^{-1})$	Fixed
ϕ	0.044737 $(year^{-1})$	Fitted
α	0.069668 $(year^{-1})$	Fitted
ν	0.014244 $(year^{-1})$	Assumed

Figure 4 provides a comprehensive comparison between the model predictions and the observed tuberculosis (TB) incidence data. Following the calibration of the model parameters using the available dataset, the simulated curve exhibits a strong agreement with the real reported cases. This close alignment reflects the accuracy of the parameter estimation process and the capability of the model to reproduce the temporal dynamics of TB transmission.

The goodness of fit is quantified by the coefficient of determination, which yields a value of $R^2 = 0.9119$. This high value indicates that the model is able to explain approximately 91.19% of the variability present in the observed data. In other words, the model captures the major trends and fluctuations in the incidence time series, demonstrating its effectiveness in representing the underlying epidemiological processes.

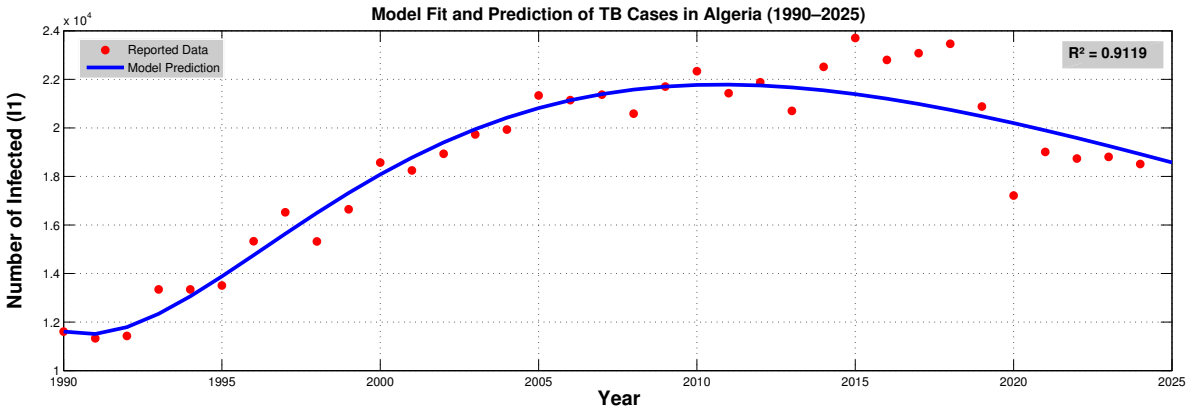

Figure 4. Model fitting to the tuberculosis case data in Algeria.

5.2. The numerical simulation without delay

In this part, we examine the stability of the model through numerical simulations in the absence of delay. Using the parameter values listed in Table 2, the basic reproduction number is calculated as $\mathcal{R}_0 = 1.20$, which aligns with the tuberculosis situation reported in Algeria. Since $\mathcal{R}_0 > 1$, the model admits a unique endemic equilibrium point, indicating that the disease remains present in the population, although its dynamics are regulated rather than uncontrolled.

Using the parameter values adopted in the numerical study, we verify that the Routh–Hurwitz condition (4.12) is fully satisfied, which confirms the local stability of the endemic equilibrium. Based on these values, the simulations show that the number of infectious individuals experiences a slight increase, while the number of recovered individuals rises in parallel. This behavior indicates that the infection persists at a controlled level, while diagnosis and treatment remain sufficiently effective to maintain a stable recovery rate. The results also highlight that the health system responds efficiently to new cases and prevents any sharp escalation in transmission. In light of this, it appears that Algeria continues to maintain control over the spread of tuberculosis despite the ongoing emergence of new infections.

Figure 5 supports this conclusion, as the system trajectories move stably toward the endemic equilibrium while the recovered population increases. This figure was generated using the classical fourth-order Runge–Kutta method, since for $\tau = 0$ the model reduces to an ordinary differential system. The resulting dynamics illustrate a controlled epidemiological situation, where the rise in recoveries effectively balances the increase in infections, ensuring that the disease remains manageable. Therefore, maintaining strong treatment programs, enhancing early diagnosis, and reinforcing public health interventions remain essential to strengthening Algeria's control over tuberculosis and limiting its long-term impact.

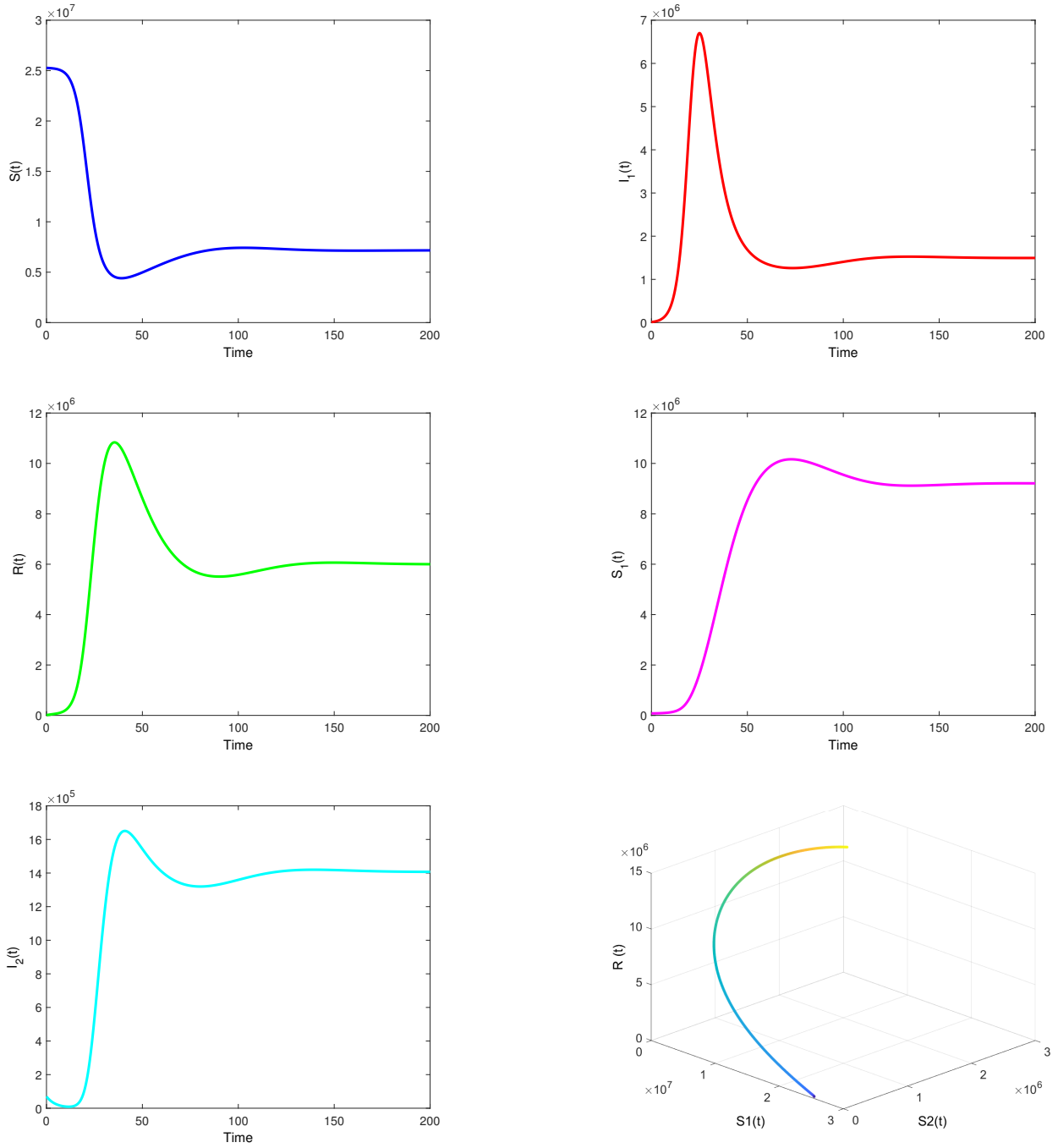

Figure 5. Time evolution of the tuberculosis model compartments in Algeria.

5.3. The numerical simulation with delay

Let us consider a hypothetical scenario in which treatment efforts decline after the year 2024, such that the population no longer receives effective medical care. This leads to a sharp decrease in the recovery rate to a very small value, for example $\gamma = 0.001$. Using all the remaining parameter values as provided in Table 2, we obtain $\mathcal{R}_0 > 1$. This means that each infected individual can, on average, transmit the disease to more than one person, leading to the persistence of the infection within the

community rather than its elimination. Moreover, the condition $\mathcal{R}_0 > 1$ is essential for the existence of an endemic equilibrium, that is, a steady state in which a nonzero number of infected individuals persists over the long term.

Using the calibrated parameter values listed in Table 2, we computed the time delay τ based on the analytical expression shown in equation (4.19). This expression allowed us to determine the critical delay value, which was found to be $\tau_0 \approx 3.4$. This value represents the threshold at which the qualitative behavior of the model begins to change significantly, noting that the time variable is expressed in years.

For delay values satisfying $0 \leq \tau < 3.4$, the endemic equilibrium remains locally stable, reflecting an epidemiological situation that remains controlled, with infection levels staying within a stable range. However, when the delay exceeds this threshold ($\tau > 3.4$), the roots of the characteristic equation cross the imaginary axis, leading to a loss of stability and the emergence of periodic solutions through a Hopf bifurcation. Epidemiologically, this phenomenon manifests as recurrent oscillations in the number of infected individuals, resembling successive waves of infection that are difficult to manage. Therefore, the critical value $\tau_0 \approx 3.4$ marks the key transition point where the system dynamics shift from stability to a periodic regime.

Figure 6 clearly illustrates the stability of the endemic equilibrium for delay values smaller than the critical threshold τ_0. Figure 6(a) shows the temporal evolution of the model variables, where all trajectories converge smoothly toward the equilibrium point, confirming local stability. Figure 6(b) presents a three-dimensional phase portrait, which further demonstrates that the solution curves spiral toward the equilibrium surface, indicating that the system remains well-behaved and asymptotically stable when $\tau < \tau_0$.

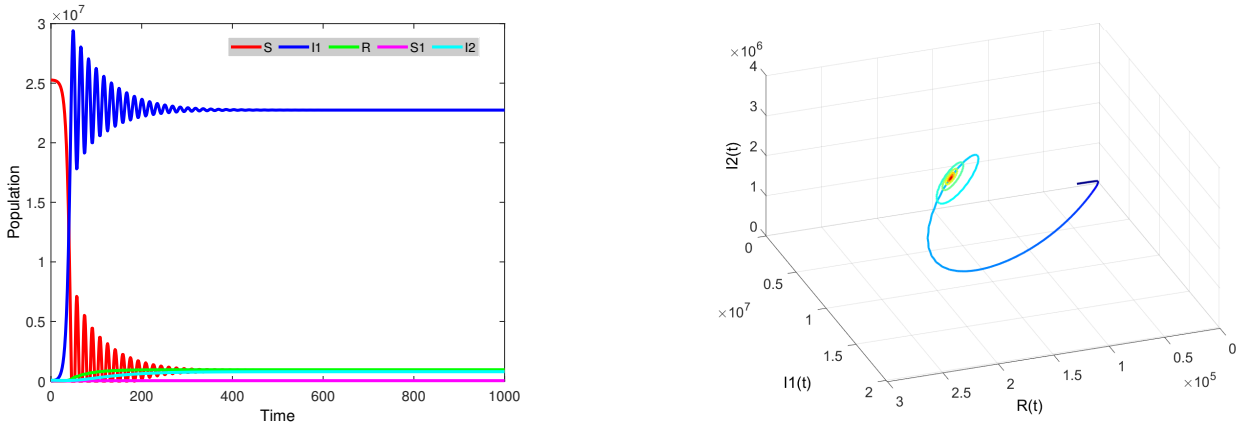

(a) Stability for $\tau < \tau_0$

(b) Phase dynamics of the system

Figure 6. The graphs demonstrate that the endemic equilibrium point E^* exhibits local asymptotic stability when $\tau < \tau_0$.

In contrast, Figure 7 (a) depicts the system dynamics when the delay exceeds the critical value τ_0. The time-series curves show persistent oscillations in the infected compartments, indicating that the endemic equilibrium loses stability and that periodic behavior emerges as a result of a Hopf bifurcation. Figure 7 (b) presents the corresponding three-dimensional trajectory, which no longer converges to the equilibrium point but instead forms a closed orbit, illustrating the appearance of a stable limit cycle. This confirms that for $\tau > \tau_0$, the system switches from a controlled endemic state to recurrent epidemic

waves.

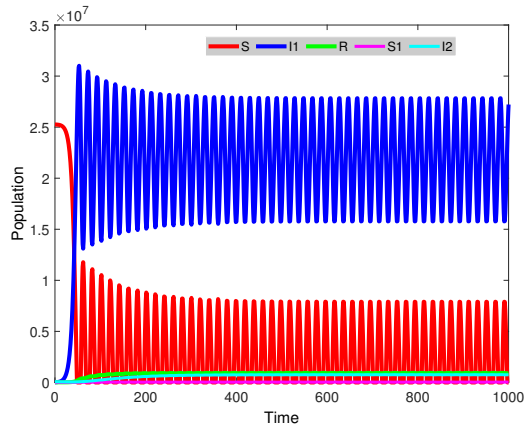

(a) Instability for $\tau > \tau_0$

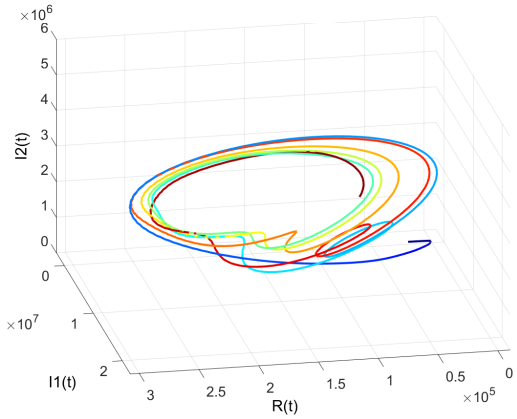

(b) 3D phase dynamics

Figure 7. The graphs show that the endemic equilibrium point E^* becomes unstable when $\tau > \tau_0$.

This scenario suggests that if the transmission rate remains high while delays in case detection exceed four years, Algeria may lose its ability to control tuberculosis after 2024, especially if early detection and rapid treatment measures are not strengthened.

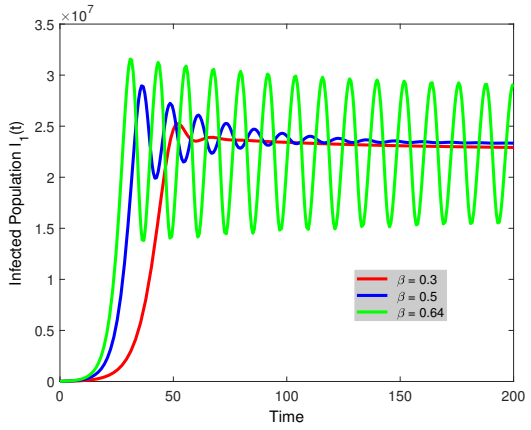

(a) Dynamics for varying β

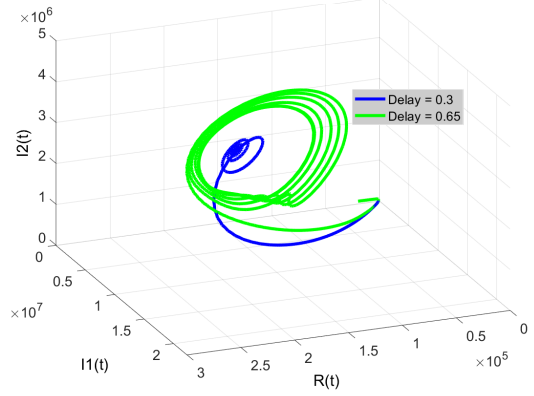

(b) 3D dynamics for varying β

Figure 8. Graphs illustrating the system dynamics for various values of β with a fixed delay $\tau = 3$.

The numerical simulation in Figure 8 (a-b) illustrates the effect of increasing the infection rate β on the dynamics of the infected population when the delay is fixed at $\tau = 3$. For moderate values such as $\beta = 0.3$, the system stabilizes rapidly, and the number of infected individuals converges smoothly to a steady endemic level. When β increases to $\beta = 0.5$, small transient oscillations appear before the solution eventually stabilizes, indicating that the system becomes more sensitive to temporal effects. For higher transmission intensity, as in the case of $\beta = 0.64$, the system loses stability and exhibits large-amplitude sustained oscillations. This persistent periodic behavior signals the onset of a Hopf

bifurcation, where the equilibrium becomes unstable and a stable limit cycle emerges. The importance of the infection rate β is clearly reflected in this behavior: Increasing β not only amplifies the number of infections but also strengthens the destabilizing influence of the delay, making the system more prone to instability and the emergence of recurrent epidemic cycles. Overall, the figure shows that higher infection rates increase the sensitivity of the system to any delay, thereby complicating the control of disease dynamics and raising the likelihood of repeated epidemic waves.

Figure 9 illustrates the temporal evolution of the model dynamics for different values of the time delay. As the delay increases, the system progressively loses stability and sustained periodic oscillations emerge, indicating the occurrence of a Hopf bifurcation. These oscillatory patterns reflect complex tuberculosis dynamics driven by delayed progression and treatment processes.

The results show that large delay values amplify fluctuations in the system, reducing its ability to return to equilibrium. In particular, prolonged delays associated with case detection and treatment initiation, together with reinfection and relapse after treatment, weaken the stabilizing effect of the treatment rate and may compromise disease control. This behavior suggests that insufficiently rapid treatment, combined with secondary infection and renewed susceptibility after recovery, can limit Algeria's capacity to control tuberculosis. These findings emphasize the importance of timely treatment, continuous monitoring, and effective post-treatment management in mitigating oscillatory disease dynamics (see Figure 9).

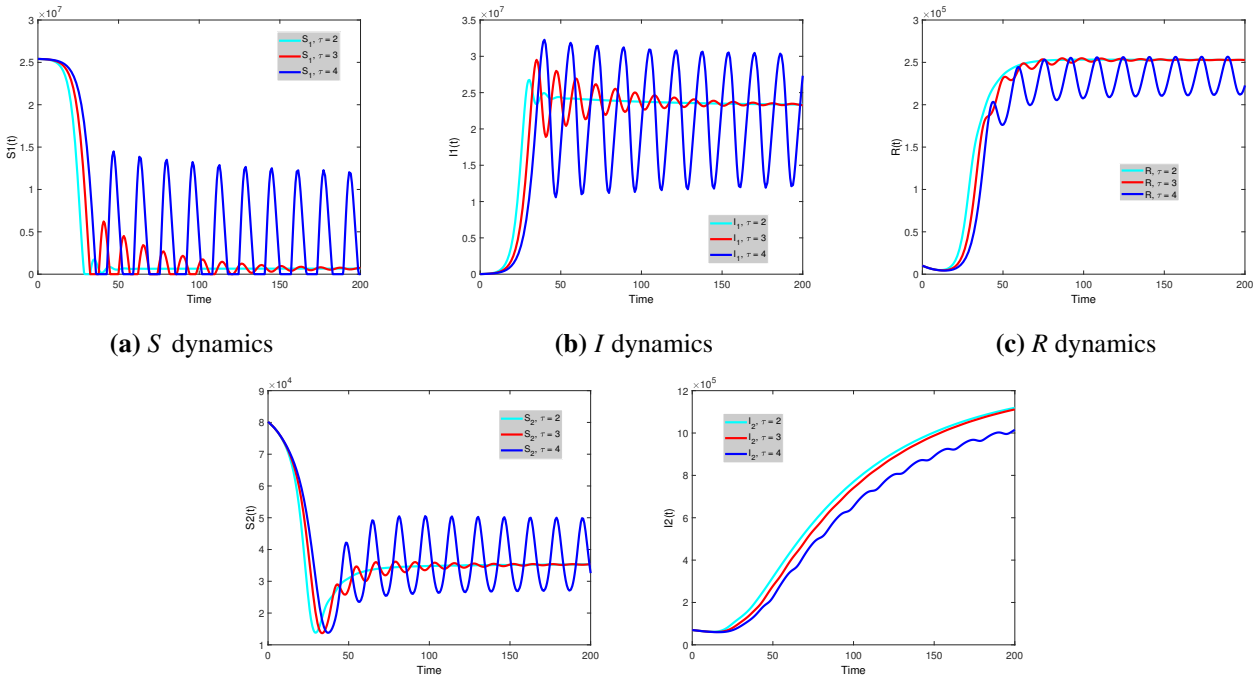

(a) S dynamics **(b)** I dynamics **(c)** R dynamics

(d) Secondary S dynamics **(e)** Secondary I dynamics

Figure 9. Oscillatory dynamics of the tuberculosis model with time delay ($\tau = 2, 3, 4$).

6. Conclusions

This study develops a nonlinear mathematical model with time delay to investigate the transmission dynamics of tuberculosis in Algeria over the period 1990–2024. By incorporating key epidemiological features such as the incubation period between infection and the onset of infectiousness, reinfection, and the loss of immunity following treatment, the model provides a realistic representation of the long-term progression and persistence of tuberculosis. The mathematical analysis confirms that the model is biologically well posed and satisfies essential epidemiological conditions, including the positivity and boundedness of solutions.

The basic reproduction number $\mathcal{R}_0$ is derived and identified as a fundamental threshold parameter governing the long-term behavior of the system. Stability analysis demonstrates that when $\mathcal{R}_0 < 1$, the disease-free equilibrium is globally stable and tuberculosis transmission cannot be sustained, whereas for $\mathcal{R}_0 > 1$, the system admits a stable endemic equilibrium, indicating persistent transmission within the population. Sensitivity analysis further highlights the most influential epidemiological parameters affecting $\mathcal{R}_0$, thereby identifying key drivers of disease spread and potential targets for intervention.

The results also show that time delay plays a critical role in shaping the system dynamics. Delays associated with disease progression, diagnosis, and treatment initiation can significantly alter stability properties and may induce complex dynamics, including periodic oscillations via Hopf bifurcation. These oscillatory patterns reflect recurrent waves of tuberculosis transmission and are consistent with observed long-term epidemiological trends of the disease.

Numerical simulations calibrated with tuberculosis data from Algeria for the period 1990–2024 support the analytical findings and clearly demonstrate the impact of delay effects on epidemic evolution. The results suggest that prolonged delays in case detection and treatment initiation can substantially weaken control efforts, even when treatment programs are in place.

From a public health perspective, these findings underscore the urgent need to strengthen early detection systems, reduce diagnostic and treatment delays, and improve treatment adherence and post-treatment monitoring to prevent relapse and reinfection. The study provides quantitative evidence that timely interventions can significantly reduce transmission and disease burden. This is particularly important for older adults, whose heightened vulnerability to severe respiratory infections was made especially evident during the COVID-19 pandemic [34]. As a direction for future research, the model can be extended to incorporate optimal control strategies, including vaccination, enhanced treatment coverage, and accelerated diagnosis as time-dependent controls. Such extensions would enable the design of cost-effective and sustainable intervention policies, offering valuable guidance for tuberculosis control programs and evidence-based public health decision-making in Algeria.

Use of AI tools declaration

The authors declare they have not used Artificial Intelligence (AI) tools in the creation of this article.

Acknowledgments

Maíra Aguiar acknowledges financial support from the Spanish Ministerio de Ciencia e Innovación (MICINN) through the Ramón y Cajal grant RYC2021-031380-I. Akhil Kumar Srivastav acknowl-

edges financial support from the Spanish Ministerio de Ciencia e Innovación (MICINN) through the Juan de la Cierva grant FJC2021-046826-I. This research was supported by the Basque Government through the "Mathematical Modeling Applied to Health" project (BERC 2022–2025 programme) and by the Spanish Ministry of Science, Innovation and Universities through the BCAM Severo Ochoa accreditation CEX2021-001142-S (MICINN/AEI/10.13039/501100011033).

Conflict of interest

The authors declare there are no conflict of interest.

References

1. *World Health Organization,* Global Tuberculosis Report 2024, WHO Press, 2024.
2. K. Lönnroth, M. Raviglione, M. Weil, P. Uplekar, M. R. Dye, K. G. Williams, et al., Tuberculosis control and elimination 2010–50: cure, care, and social development, *Lancet* **375** (2010), 1814–1829. https://doi.org/10.1016/S0140-6736(10)60483-7
3. F. Brauer, C. Castillo-Chavez, Mathematical Models in Population Biology and Epidemiology, Springer, Berlin, 2012. https://doi.org/10.1007/978-1-4614-1686-9
4. A. Nabti, S. Djilali, S. Bentout, Stability and spatial profiles of a double age-dependent diffusive viral infection model with spatial heterogeneity, *Z. Angew. Math. Phys.* **76** (2025), 89. https://doi.org/10.1007/s00033-025-02466-1
5. H. Y. Lam, S. Jayasinghe, K. D. Ahuja, A. P. Hills, Agent-based modelling in active commuting research: A scoping review, *Crit. Public Health* **35** (2025), 2483473. https://doi.org/10.1080/09581596.2025.2483473
6. A. Nabti, M. Kirane, Global dynamics of an age-structured tuberculosis model with a general nonlinear incidence rate, *J. Biol. Syst.* **33** (2025), 1117–1159. https://doi.org/10.1142/S0218339025500330
7. R. Chinnathambi, F. A. Rihan, H. J. Alsakaji, A fractional-order model with time delay for tuberculosis with endogenous reactivation and exogenous reinfections, *Math. Methods Appl. Sci.* **44** (2021), 8011–8025. https://doi.org/10.1002/mma.5676
8. S. Bhatter, A. K. Verma, R. K. Upadhyay, M. A. Khan, S. Kumar, P. Singh, Mathematical modeling of tuberculosis using Caputo fractional derivative: a comparative analysis with real data, *Sci. Rep.* **15** (2025), 12672. https://doi.org/10.1038/s41598-025-12672-3
9. A. Ghanmi, A. Nabti, Stability study for an age-structured epidemic model with latent phase, relapse and nonlinear infection rate, *Mathematics* **13** (2025), 3994. https://doi.org/10.3390/math13243994
10. K. L. Cooke, P. van den Driessche, On zeroes of some transcendental equations, *Funkc. Ekvacioj* **29** (1986), 77–90.
11. A. K. Srivastav, M. Ghosh, Modeling the transmission dynamics of malaria with saturated treatment: A case study of India, *J. Appl. Math. Comput.* **67** (2021), 519–540. https://doi.org/10.1007/s12190-020-01416-9

12. Y. Kuang, Delay Differential Equations with Applications in Population Dynamics, Academic Press, New York, 1993. https://doi.org/10.1016/C2009-0-22254-6
13. N. Abidat, A. Nabti, K. Bouaziz, Hopf bifurcation analysis of a TB infection model with two discrete time delays, *Palest. J. Math.* **14** (2025). https://pjm.ppu.edu/vol/2220
14. W. M. Liu, H. W. Hethcote, S. A. Levin, Dynamical behavior of epidemiological models with nonlinear incidence rates, *J. Math. Biol.* **25** (1987), 359–380. https://doi.org/10.1007/BF00277162
15. A. Nabti, Dynamical analysis of an age-structured SEIR model with relapse, *Z. Angew. Math. Phys.* **75** (2024), 84. https://doi.org/10.1007/s00033-024-02227-6
16. E. Beretta, Y. Kuang, Geometric stability switch criteria in delay differential systems with delay-dependent parameters, *SIAM J. Math. Anal.* **33** (2002), 1144–1165. https://doi.org/10.1137/S0036141000376086
17. Algerian Ministry of Health, National Report on Tuberculosis Control in Algeria., *Ministry of Health Publications,* 2023.
18. Ministry of Health Algeria, National Tuberculosis Report 2023, *Ministère de la Santé,* (2023).
19. *World Health Organization,* Global Tuberculosis Report 2024, WHO Press, 2024.
20. *World Health Organization,* Treatment of Tuberculosis: Guidelines for National Programmes., WHO Press, 1997.
21. S. Saha, P. Dutta, G. Samanta, Dynamical behavior of SIRS model incorporating government action and public response in presence of deterministic and fluctuating environments, *Chaos Solitons Fractals* **164** (2022), 112643. https://doi.org/10.1016/j.chaos.2022.112643
22. P. Dutta, G. Samanta, J. J. Nieto, Periodic transmission and vaccination effects in epidemic dynamics: a study using the SIVIS model, *Nonlinear Dyn.* **112** (2024), 2381–2409. https://doi.org/10.1007/s11071-023-08967-5
23. S. Dutta, P. Dutta, P. Akhtar, G. Samanta, Bifurcation analysis and chaotic dynamics in an SIR model with nonlinear incidence and constrained healthcare capacity, *Chaos Solitons Fractals* **201** (2025), 117329. https://doi.org/10.1016/j.chaos.2025.117329
24. *World Health Organization,* Global Tuberculosis Report 2023, WHO Press, Geneva, 2023.
25. Z. Feng, C. Castillo-Chavez, A. F. Capurro, A model for tuberculosis with exogenous reinfection, *Theor. Popul. Biol.* **57** (2000), 235–247. https://doi.org/10.1006/tpbi.2000.1451
26. C. Castillo-Chavez, Z. Feng, To treat or not to treat: the case of tuberculosis, *J. Math. Biol.* **35** (1997), 629–656. https://doi.org/10.1007/s002850050069
27. P. van den Driessche, J. Watmough, Reproduction numbers and sub-threshold endemic equilibria for compartmental models of disease transmission, *Math. Biosci.* **180** (2002), 29–48. https://doi.org/10.1016/S0025-5564(02)00108-6
28. N. Chitnis, J. Hyman, J. M. Cushing, Determining important parameters in the spread of malaria through the sensitivity analysis of a mathematical model, *Bull. Math. Biol.* **70** (2008), 1272–1296. https://doi.org/10.1007/s11538-008-9299-0
29. E. O. Alzahrani, W. Ahmad, M. A. Khan, S. J. Malebary, Optimal control strategies of Zika virus model with mutant, *Commun. Nonlinear Sci. Numer. Simul.* **93** (2021), 105532. https://doi.org/10.1016/j.cnsns.2020.105532

30. W. Rudin, Principles of Mathematical Analysis, McGraw-Hill, New York, 1976.
31. T. Tao, Analysis II, Springer, 2016. https://doi.org/10.1007/978-981-10-1804-6
32. WHO. *Global Tuberculosis Report*; World Health Organization: Geneva, Switzerland, 2023. Available from: `https://extranet.who.int/tme/generateCSV.asp?ds=notifications`
33. World Bank, Population, total – Algeria, Available from: `https://data.worldbank.org/indicator/SP.POP.TOTL?locations=DZ`
34. M. Aguiar, N. Stollenwerk, Condition-specific mortality risk can explain differences in COVID-19 case fatality ratios around the globe, *Public Health* **188** (2020), 18–20. https://doi.org/10.1016/j.puhe.2020.08.004

AIMS Press

© 2026 the Author(s), licensee AIMS Press. This is an open access article distributed under the terms of the Creative Commons Attribution License (https://creativecommons.org/licenses/by/4.0)